

A REAPPRAISAL OF THE GENUS *LEPTOCYLINDRUS* (BACILLARIOPHYTA), WITH THE ADDITION OF THREE SPECIES AND THE ERECTION OF *TENUICYLINDRUS* GEN. NOV.¹

Deepak Nanjappa, Wiebe H. C. F. Kooistra, and Adriana Zingone²

Ecology and Evolution of Plankton Laboratory, Stazione Zoologica Anton Dohrn, Villa Comunale, Naples 80121, Italy

Centric diatoms of the genus *Leptocylindrus* are common in the marine plankton worldwide. Only two species, *L. danicus* Cleve and *L. minimus* Gran, so far clearly belong to this genus, whose diversity has not been fully investigated. We investigated frustule and spore morphology as well as three nuclear- and three plastid-encoded markers of 85 *Leptocylindrus* strains from the Gulf of Naples, and one from the Atlantic US. The strains grouped into five molecularly distinct species with different levels of morphological differentiation. Two species matched the description of *L. danicus* and produced similar spores but differed in morphometric characters and sub-central pore position, supporting the description of *L. hargravesii* Nanjappa and Zingone as a distinct species. *Leptocylindrus danicus* var. *apora* French III and Hargraves, lacking a sub-central pore and not forming spores, was raised to the species level as *L. aporus* (French III and Hargraves) Nanjappa and Zingone. A fourth species with convex valves was described as *L. convexus* Nanjappa and Zingone. The fifth species matched the description of *L. belgicus* Meunier, considered as synonym of *L. minimus*. However, ultrastructural differences from all other *Leptocylindrus* supported the erection of the genus *Tenuicylindrus* Nanjappa and Zingone with *T. belgicus* (Meunier) Nanjappa and Zingone as type species. None of the sequences matched the *L. minimus* sequence in GenBank. The species analyzed showed different or partially overlapping seasonal distributions. Despite the addition of the new taxa, the ancient diatom lineage of the Leptocylindraceae shows a relative species poorness and considerable morphological stasis.

Key index words: Diatom; Gulf of Naples; *Leptocylindrus*; LTER-MC; morphology; phylogeny; resting stages; taxonomy; *Tenuicylindrus*

Abbreviations: CBC, compensatory base changes; GoN, Gulf of Naples; HCBC, hemi-compensatory base changes; LTER-MC, Long-Term Ecological Research MareChiara; ML, Maximum Likelihood; MP, Maximum Parsimony; PAUP, Phylogenetic

Analysis Using Parsimony; SZN, Stazione Zoologica Anton Dohrn Naples

Diatom diversity is not distributed homogeneously across the phylogenetic tree. The pennates, and particularly some raphid pennate genera such as *Pseudonitzschia* Peragallo (Lundholm et al. 2012 and literature therein) and *Sellaphora* Mereschowsky (Evans et al. 2008), constitute by far the most diverse group. Mediophyceae appear to be less diverse, but several genera in this class, e.g. *Chaetoceros* Ehrenberg (Rines and Hargraves 1990, Kooistra et al. 2010), *Thalassiosira* Cleve (Beszteri et al. 2007) and *Skeletonema* Greville (Sarno et al. 2005, 2007, Zingone et al. 2005, Alverson et al. 2007, Kooistra et al. 2008), show considerable diversity as well. Cryptic and semi-cryptic species in these genera are usually closely related, showing a marked differentiation only in rapidly evolving genetic markers such as the nuclear large sub-unit (LSU) or the internal transcribed spacers (ITS) of the nuclear ribosomal RNA cistron. In contrast, the radial centric group, which is the first one to emerge in the fossil record (Gersonde and Harwood 1990), appears to include a more restricted number of generally scarcely diverse genera. The latter could be a real feature of the genera in this group or the result of limited taxonomic assessment. For instance, detailed molecular and morphological investigations revealed marked diversity in the genus *Aulacoseira* (Edgar and Theriot 2004).

Among these apparently ancient diatom lineages, the marine planktonic genus *Leptocylindrus*, the only member of the family Leptocylindraceae and of the order Leptocylindrales, exhibits a relatively simple morphology. Its species have cylindrical cells with two or more plastids and valves without conspicuous processes or complex ornamentations. Molecular phylogenies at times resolve the genus as sister to a clade containing most or all other diatoms (Sorhannus 2004). Currently, two main species are widely recognized: *L. danicus* Cleve (1889), with its variety *L. danicus* var. *apora* French III and Hargraves (1986), and *L. minimus* Gran (Gran 1915, see also Hargraves 1990, Rivera et al. 2002). The taxonomic affiliation of a third species, *L. mediterraneus* (H. Peragallo) Hasle, has been questioned (Hasle and Syvertsen 1997, Gomez 2007). In fact, only empty frustules with ultrastructural features distinct from

¹Received 7 December 2012. Accepted 23 May 2013.

²Author for correspondence: e-mail: zingone@szn.it.
Editorial Responsibility: K. Valentin (Associate Editor)

those of other *Leptocylindrus* species are observed in nature, almost always colonized by the protozoan *Solenicola setigera* Pavillard (Gomez 2007). Two other described species, namely *L. belgicus* Meunier (Meunier 1915) and *L. adriaticus* Schröder (1908), have been considered subsequently as synonym of *L. minimus* (Hustedt 1962, Hendey 1964), and variety of *L. danicus* (Schiller 1929), respectively. The identity of *L. curvatus* (Skvortzow 1931), based on a drawing of an undulated chain of cells with small plastids, remains uncertain and has hardly been followed by any subsequent report. A further species, *L. maximus*, was reported by Smayda (1963) from the Gulf of Panama, but it has never been described. So far, no thorough morphological and molecular taxonomic study of this genus has been undertaken and only one nuclear SSU rDNA sequence for a strain of *L. danicus* (AJ535175) and one for a strain of *L. minimus* (AJ535176) are available in GenBank to date.

Life cycles show a considerable disparity among *Leptocylindrus* species. Murray et al. (1912) described the formation of highly silicified resting spores in *L. danicus* and Gran (1915) reported that these resting spores develop directly from auxospores. Subsequently, Davis et al. (1980) and French and Hargraves (1985, 1986) demonstrated the formation of resting spores in in vitro cultures, confirming that *L. danicus* is one of the few diatom species forming these markedly distinct stages following sexual reproduction. In contrast, the variety *L. danicus* var. *apora* restores its cell size by vegetative cell enlargement (French and Hargraves 1986). Instead *L. minimus* was found to form resting stages during the vegetative growth, which is similar to what happens in the life cycles of most other planktonic diatoms (Hargraves 1990).

Leptocylindrus danicus has been reported throughout the world's oceans, except in Arctic waters, and forms major blooms in coastal waters. *L. minimus* has been reported from the Mediterranean Sea, along the North Atlantic coasts of Europe and America as well as in the eastern and western South Pacific (Intergovernmental Oceanographic Commission (I.O.C) UNESCO (2012). In the GoN (Tyrrhenian Sea, Mediterranean Sea), specimens assignable to *L. danicus* are observed throughout the year (Ribera d'Alcalà et al. 2004), with two distinct bloom phases, a conspicuous one in summer and a more modest one in autumn. *L. minimus* is recurrently found in autumn. *L. mediterraneus* is also present in the GoN but will not be considered in this study, given the above mentioned taxonomic uncertainties and lack of cultured material.

The aim of this study was to investigate the diversity of the genus *Leptocylindrus* in the GoN by combining morphological and molecular data with information on the life cycle. To this end, a series of strains of *Leptocylindrus* isolated from the GoN over an entire seasonal cycle were examined using six molecular markers as well as with light- and elec-

tron microscopy. In addition, spore induction studies were conducted to elucidate the life cycle patterns in the taxa investigated. The overall aim was to test whether this apparently ancient genus is actually species poor or far more diverse than currently perceived. Based on our results, two new species, *L. hargravesii* and *L. convexus* are described and the taxon *L. danicus* var. *apora* is raised to the rank of species. In addition, the new genus *Tenuicylindrus* is established within the Leptocylindraceae including a single species *T. belgicus* (Meunier) Nanjappa and Zingone.

METHODS

Strain isolation. Eighty-six strains were obtained to assess the morphological and genetic diversity of *Leptocylindrus* (Table S1 in the Supporting Information). Single cells or chains were gathered from net samples collected at the LTER-MC in the GoN (40.80° N, 14.25° E) from October 2009 to February 2011. Strain CCMP 1856 was obtained from the National Centre for Marine Algae and Microbiota (NCMA; formerly CCMP). Single cells or short chains of *L. danicus* were isolated using drawn-out Pasteur pipettes and grown into unialgal strains in 70 mL polystyrene culture flasks containing 30 mL of sterile K medium (Keller et al. 1987) prepared with locally collected oligotrophic seawater. Cultures were maintained at 20°C, 60 $\mu\text{mol photons} \cdot \text{m}^{-2} \cdot \text{s}^{-1}$ and a 12:12 light:dark (L:D) cycle.

Microscopic observations. Microscopic observations were made on selected strains including representatives of each genetically distinct group. Morphological features were observed in LM, TEM, and SEM. Ultrastructural morphometric data were obtained in TEM and SEM. All LM observations were carried out on exponentially growing cultures and natural samples from the GoN (St. LTER-MC) using a Zeiss Axiophot microscope (Carl Zeiss, Oberkochen, Germany) equipped with Nomarski differential interference contrast (DIC), phase contrast, and bright-field optics. Light micrographs were taken using a Zeiss Axiocam digital camera.

For TEM preparation, samples from exponential cultures were treated with acids (1:1:4, sample: HNO_3 : H_2SO_4), boiled for a few minutes, and then washed with distilled water for many times. Acid cleaned material was mounted on Formvar-coated grids and examined under a TEM LEO 912AB (LEO, Oberkochen, Germany). Permanent mounts were made by mounting the dry clean material in Hyrax (Hasle 1978). For SEM preparation, samples were dehydrated by increasing percentage of ethanol and then passed through critical point drying (Polaron E3000 Series II, Thermo Scientific, Milan, Italy), sputter coated with gold-palladium using a SC7640 Auto/Manual High Resolution Sputter Coater (Polaron Thermo Scientific, Milan, Italy) and observed using a JEOL JSM-6500F SEM (JEOL-USA Inc., Peabody, MA, USA).

DNA extraction, PCR amplification, sequencing, and phylogenetic analyses. Exponentially growing cultures (density of 50×10^3 cells $\cdot \text{mL}^{-1}$) were harvested by centrifugation (20,800 g at 15°C for 10 min) and DNA was extracted using a CTAB protocol as described in (Kooistra et al. 2003). The following markers of the nuclear ribosomal RNA-coding cistron were amplified: the SSU (18S) rDNA, the Internal Transcribed Spacer region (ITS1, 5.8S rDNA and ITS2) and ca. 700 bp of the 5'-end of the LSU rDNA; of the plastidial DNA were amplified the SSU (16S) rDNA, the Rubisco-large sub-unit (*rbcL*), and the photosystem II binding complex (*psbC*) following polymerase chain reaction (PCR) protocols and

amplification primers as listed in Table S2 in the Supporting Information. The PCR products were purified using a QIAquick gel extraction kit (Qiagen, Milan, Italy) according to the manufacturer's instructions. Purified products were analyzed on an automated Capillary Electrophoresis Sequencer "3730 DNA Analyzer" (Applied Biosystems, Carlsbad, CA, USA). Sequencing primers are also listed in Table S2.

To determine the phylogenetic relationships among the strains of *Tenuicylindrus* and *Leptocylindrus*, homologous sequences of the nuclear SSU rDNA, ITS and partial LSU rDNA, plastid SSU rDNA, *psbC* and *rbcl* were aligned using the Clustal-W multiple alignment module (Thompson et al. 1994) in Bioedit v. 7.1.3 (Hall 1999) and the obtained alignments adjusted, if needed, by eyeball using the sequence alignment editor Se-Al version 2.0a11 (Rambaut 1996–2002). ML trees were constructed utilizing PAUP* (Phylogenetic Analyses Using Parsimony; version 4.0 and other methods; Swofford 1998). Prior to ML analysis, identical sequences were removed from the alignments until only pairs of identical sequences remained.

ML trees were obtained as follows. Modeltest version 3.06 (Posada and Crandall 2001) was used to select optimal base substitution models and values for base composition, % invariable sites, and gamma shape parameter according to the Akaike information criterion. ML analyses were performed under the full heuristic search option in PAUP* version 4.0b10 and were constrained with values obtained by Modeltest. Trees were started by random stepwise addition and tree-bisection-reconnection branch-swapping, performing ten replicate runs. Only best trees were kept. Bootstrap values associated to internodes were based on 1,000 bootstrap replicates; each replicate was carried out as described for heuristic searches with a single run per bootstrap replicate. Resulting trees were depicted using *Tenuicylindrus* as outgroup. Heuristic searches in MP were carried out by keeping best trees only; trees were started by random stepwise addition and tree-bisection-reconnection branch-swapping, performing ten replicate runs (trees not shown). Synapomorphies along each of the branches were mapped over the respective ML trees.

The position of *Leptocylindrus* and *Tenuicylindrus* in the phylogeny of the diatoms was also verified by aligning the nuclear-encoded SSU rDNA, the plastid-encoded *rbcl* and *psbC* sequences of these genera with a concatenated data set including sequences of the same markers from other diatoms and *Bolidomonas* (data matrix S10953, downloaded from <http://www.treebase.org>; Theriot et al. 2010). Taxa for which one or more of the three sequences were missing were removed from this alignment. ML trees of the three marker regions separately as well as the concatenated sequences were inferred using RAxML-VI-HPC (Stamatakis 2006) using the following settings: substitution model, GTR-GAMMA; algorithm executed, hill-climbing; 100 alternative bootstrap runs on distinct starting trees; bootstrap random seed-option (other options not modified). Resulting trees were visualized and edited in Dendroscope (Huson and Scornavacca 2012).

The secondary structure of ITS regions was predicted using the *RNAfold* webserver (Hofacker et al. 1994), which was also used to identify CBCs and HCBCs. Helices were compared with each other to identify possible homologous regions to assist alignment.

Sequence dissimilarity within the Leptocylindraceae was assessed for the nuclear encoded SSU rDNA, the hypervariable ca 700 base pairs at the 5'-end of the LSU rDNA as well as the plastid encoded *rbcl* and *psbC*. The same was performed for *Aulacoseira*, *Chaetoceros* and *Bacteriastrum*, *Skeletonema*, *Pseudonitzschia* and *Sellaphora* by performing a nucleotide BLAST (<http://blast.ncbi.nlm.nih.gov/Blast.cgi>) of a query sequence on the nucleotide collection using a BLAST algorithm opti-

mized for "somewhat similar sequences". Resulting output was queried for the smallest maximum identity (largest dissimilarity) value of a sequence within the genus given a query-coverage of $\geq 96\%$.

Spore induction. For an explicit description of the identity of different species, it is important to elucidate the differences in the life cycle patterns, in particular the sexual reproductive stage. Spore induction studies were carried out with two strains representative of each genetically distinct clade (Table S1). Sexual reproduction experiments were carried out in "T" medium as described in French and Hargraves (1980) (f/2 medium [Guillard and Ryther 1962] with reduced nutrient concentrations) at 16°C using cool fluorescent light of 80 $\mu\text{mol photons} \cdot \text{m}^{-2} \cdot \text{s}^{-1}$ intensity and a 12:12 L:D cycle. The strains submitted to these reduced nutrient conditions (Table S1) were observed regularly in the LM for 20 d. On cultures where spore formation was observed, pictures were taken in the LM and samples were prepared for SEM observations as described above.

RESULTS

Genus *Leptocylindrus* Cleve **emend.** Nanjappa and Zingone

Cells cylindrical, generally joined by their valve faces forming filamentous chains. Plastids few to many and of variable shape. Valves face convex or concave, with a central annulus delimiting a group of poroids. Sub-central pore at times present. Poroid areolae in radiating striae. Mantle curved, with poroid areolae in parallel striae. Short triangular, often blunt flap-like processes along a ring at the margin between valve face and mantle. Copulae in the girdle consisting of elongated, nearly trapezoidal half bands, with rows of areolae along their short axis.

Leptocylindrus aporus (French III and Hargraves) Nanjappa and Zingone, **comb. nov.** (Fig. 1, A–H)

Basionym: *L. danicus* var. *apora* French III and Hargraves 1986, *J. Phycol.* Phycological Society of America, USA, 22: 415–416, figure 6j.

Emended diagnosis: Cells 3.5–10.6 μm in diameter, 12.5–33 μm in pervalvar length, solitary or forming short filamentous chains. Plastids few to many, generally ovoidal. Valves with a central annulus delimiting a group of poroids, without sub-central pore. Valve face with poroid areolae (10–14 in 1 μm) in radiating striae (10–23 striae in 1 μm). Mantle curved, with poroid areolae in parallel striae (8–10 striae in 1 μm). Copulae elongated and nearly trapezoidal, with rows of areolae along their short axis. Resting spores not observed.

Holotype: Figure 6j, French and Hargraves 1986, p. 416.

Epitype: Strain SZN-B650 (Fig. 1, A–H), collected on 21 December 2010 at the LTER-MC station in the GoN (40.80° N, 14.25° E). A permanent slide is deposited at the SZN Museum as slide no. SZN-B650-01.

Additional description: The cells are 4–7.5 μm in material from the GoN and form filamentous chains of up to 24 cells (Table S3 in the Supporting

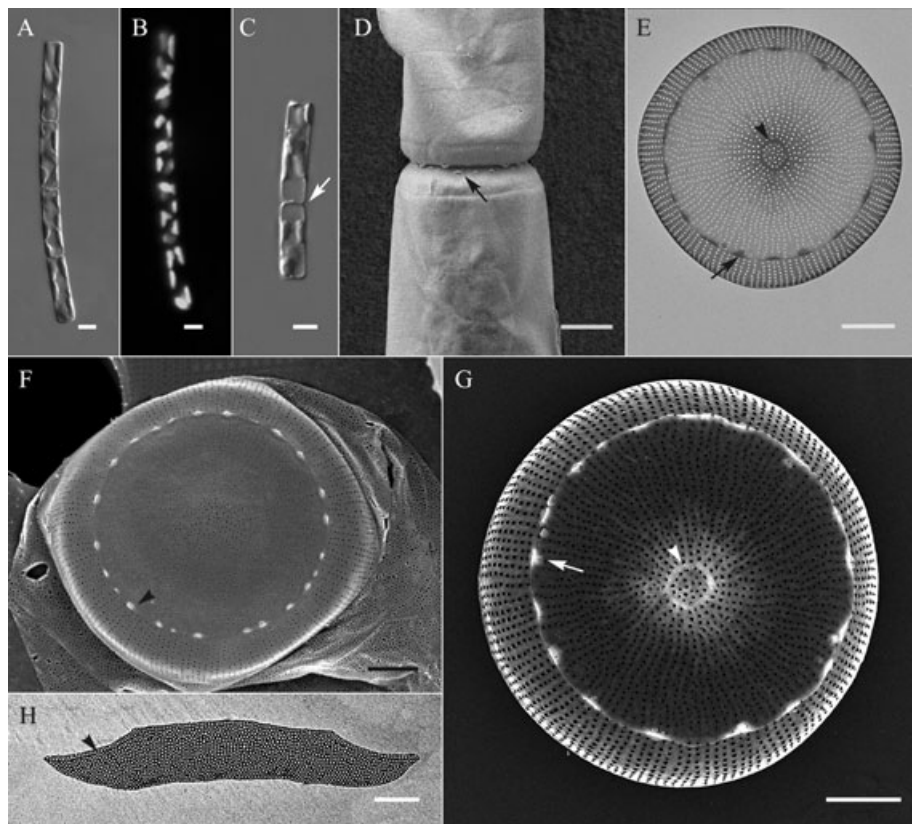


FIG. 1. *Leptocylindrus aporus*, strain SZN-B651 (A–D, F–H) and strain SZN-B743 (E). LM, DIC: A and C; epifluorescence: B. SEM: D and F. TEM: G, E and H. (A) Chain of four cells; scale bar, 5 μ m. (B) Same chain as in A, note the shape of the plastids; scale bar, 5 μ m. (C) Chain of two cells, note the shape of the joining (arrow); scale bar, 5 μ m. (D) Detail of two sibling cells in lateral view, joined by the valve face, with flaps alternating along the marginal ring (arrow). (E) Valve with central annulus (arrowhead) and blunt triangular marginal flaps (arrow); note the absence of the sub-central pore; scale bar, 1 μ m. (F) Cell in valve view, with flaps (arrowhead) at the boundary between valve face and mantle; scale bar, 1 μ m. (G) Valve with central annulus (arrowhead) and blunt triangular marginal flaps (arrow); note the absence of the sub-central pore; scale bar, 1 μ m. (H) Copula with a trapezoidal shape and an almost continuous hyaline ridge close to one border (arrowhead); scale bar, 1 μ m.

Information). Solitary cells are also often found in both culture and nature. Each cell contains 3–13 plastids (even one or two in natural samples during summer), which are ovoid and rarely discoid or elongated and are distributed along the periphery of the cell (Fig. 1, A–C). The valve faces are slightly convex or concave and show a slightly denser central area with a group of areolae delimited by a thickened hyaline annulus (Fig. 1E). The striae radiate from the central annulus toward the edge of the valve face, where the areolae become less dense and smaller (Fig. 1, E, G, and Table S4 in the Supporting Information). The valve surface is smooth except for the ring of flap-like triangular processes at the border between valve face and mantle (Fig. 1, D–G). The valve mantle is smooth and has parallel striae of round to rectangular areolae (Fig. 1, F and G). The mantle evenly curves from the valve face toward the valvocopula (Fig. 1, E–G). In the girdle, the copulae are nearly trapezoidal half bands which show a thin hyaline ridge running parallel and close to the margins of the three shorter sides of the band, delimiting one or a few parallel rows of areo-

lae (Fig. 1H). At times, the ridge is only visible along the two oblique sides of the band. Crosswise-oriented striae are present on the bands at a density of 11–16 in 1 μ m, becoming less regular and dense toward the ridge (Fig. 1H). Vegetative cell enlargement occurred in cultures growing at constant rate through globular “auxospore-like structures,” similar to those reported by French and Hargraves (1986). No spore formation was observed under nutrient depletion conditions.

***Leptocylindrus convexus* Nanjappa and Zingone, sp. nov.** (Fig. 2, A–J)

Diagnosis: Cells 3–8 μ m in diameter, 22–65 μ m in perivalvar length, forming filamentous chains or often found in couplets. Plastids few, ellipsoidal-lanceolate and elongated along the perivalvar axis, often located in the central part of the cell. Valve faces with an irregular central annulus, at times not visible, delimiting a number of areolae in the center of the valve face. No distinct sub-central pore. Poroid areolae (10–14 in 1 μ m) on the valve face in radiating striae (10–14 in 1 μ m). Mantle wide, slanting abruptly from the valve face margin toward the

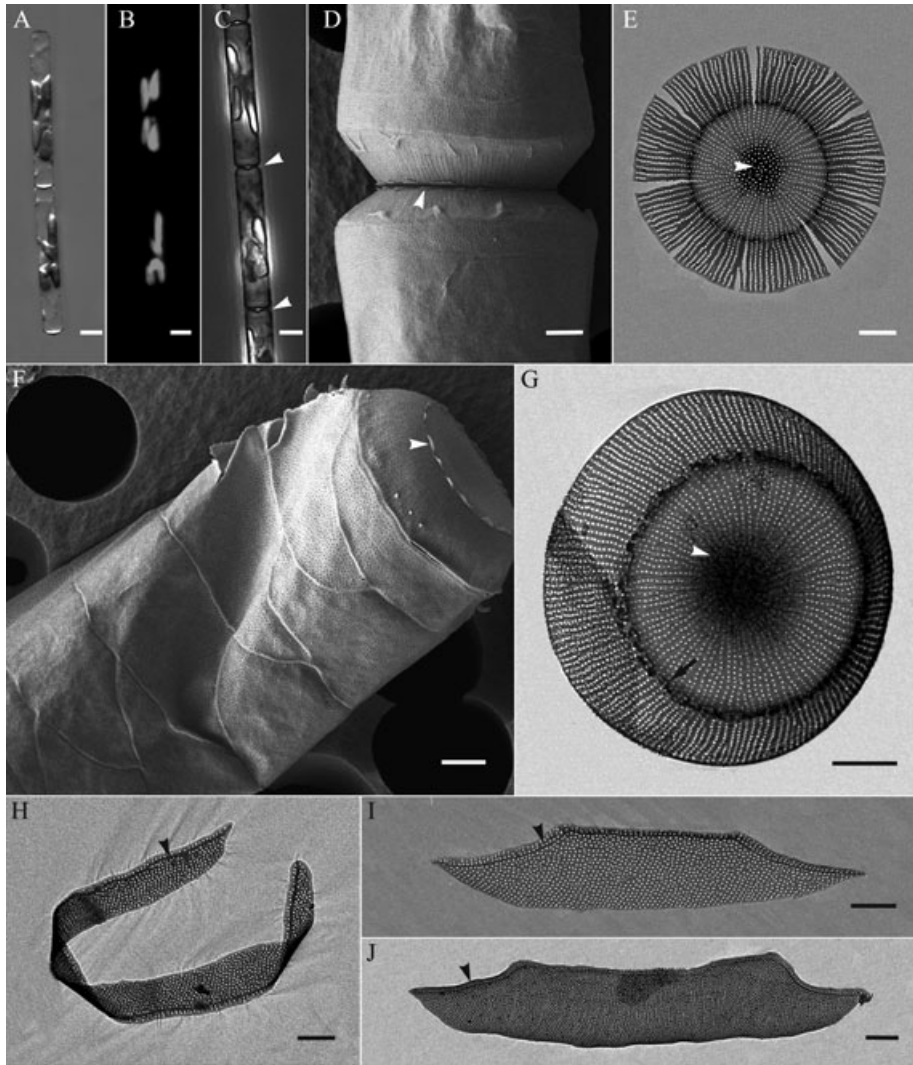


FIG. 2. *Leptocylindrus convexus*, strain SZN-B768. LM, DIC: A; LM, epifluorescence: B; LM, phase contrast: C. SEM: D and F. TEM: E, G–I and J. (A) Chain of two cells; scale bar, 5 μm . (B) Same chain as in A; note the shape of the plastids; scale bar, 5 μm . (C) Fragment of a chain; note the marked constriction at the cell joining (arrowheads); scale bar, 5 μm . (D) Details of two sibling cells joined by the valve face; note the wide mantle and the flaps in alternated position at the border of the valve faces (arrowhead); scale bar, 1 μm . (E) Valve with mantle breaks due to the marked convexity; note the absence of sub-central pore and the presence of a faint annulus (arrowhead); scale bar, 1 μm . (F) Detail of a cell in girdle view, with flaps (arrowhead) around the valve face, convex mantle and broad, pointed copulae; scale bar, 1 μm . (G) Valve with an almost continuous ring of flaps (arrow) and heavily silicified central area (arrowhead); scale bar, 1 μm . (H, I and J) Nearly trapezoidal copulae, with different size and shape; note the almost continuous hyaline line close to the borders (arrowheads); scale bar, 1 μm .

valvocopula, with areolae in parallel rows (8–11 in 1 μm). Copulae elongated and nearly trapezoidal, with irregular crosswise rows of areolae. Resting spores not observed.

Holotype. Strain SZN-B768 (Fig. 2, A–J), collected on December 21, 2010 at the LTER-MC station in the GoN (40.80° N, 14.25° E). A permanent slide is deposited at the SZN Museum as slide no. SZN-B768-01.

Etymology. The species epithet *convexus* (convex) refers to the shape of the valve.

Additional description. The cells form filamentous chains generally of 2 or 3 cells (Fig. 2, A–C;

Table S3). Chains of up to 68 cells were occasionally observed, at times in gently undulated or rarely spiralling chains. Each cell possesses few (3–11), linear or elliptical-lanceolate plastids (Fig. 2, A–C) up to 10–14 μm long in thin (3–4 μm diameter) cells. The plastids are often arranged in a star-like pattern around the central nucleus (Fig. 2C). Valve faces are either convex or concave, with a markedly silicified central part and an irregular, hardly visible annulus (Fig. 2, E and G). The striae radiating from the central part of the valve generally continue across the mantle, where they run in parallel rows of round to rectangular areolae (Fig. 2, E and G;

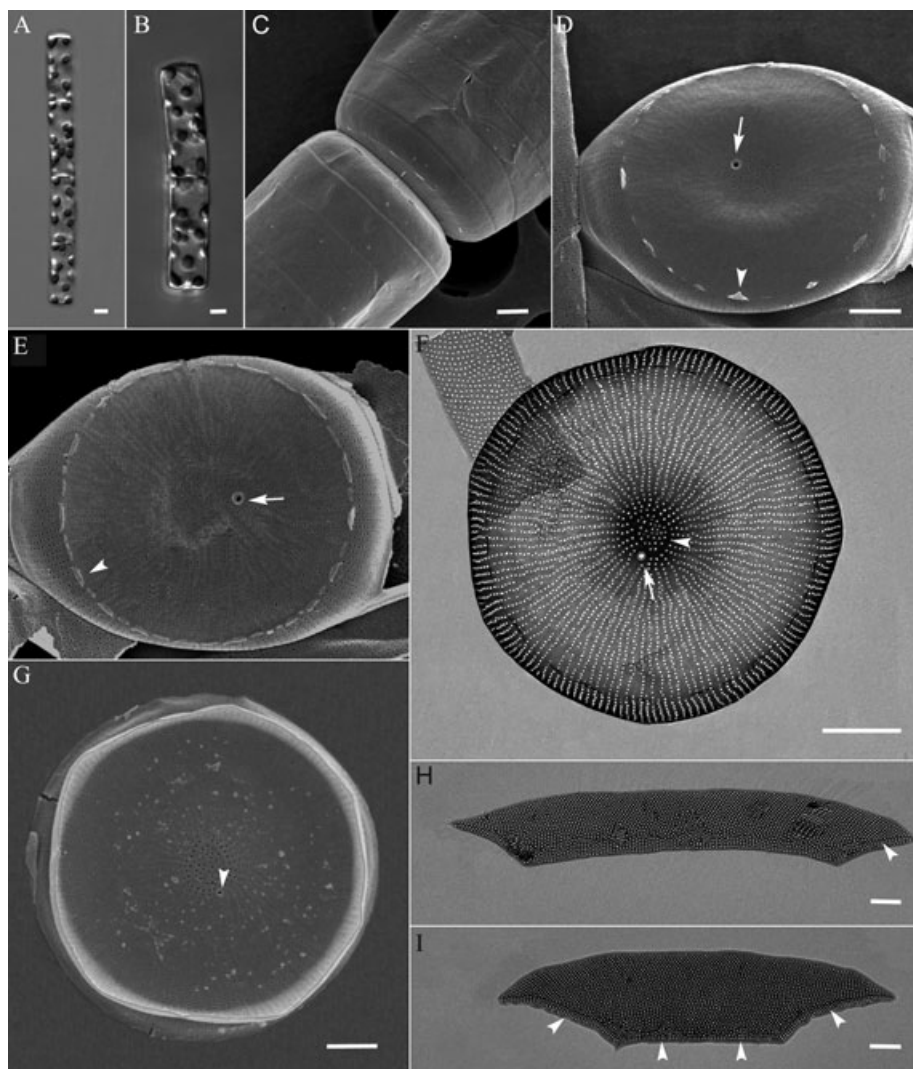


FIG. 3. *Leptocylindrus danicus*, strain SZN-B650. LM, DIC: A and B. SEM: C–E and G. TEM: F, H and I. (A) Chain of four cells; scale bar, 5 μm . (B) Chain of two cells showing the convex or concave valve surface and discoidal plastids; scale bar, 5 μm . (C) Detail of two cells joined by the valve face, with hardly visible flaps; scale bar, 1 μm . (D) Cell in valve view, with sub-central pore (arrow) and spaced triangular flaps (arrowhead); scale bar, 1 μm . (E) Cell in valve view, with sub-central pore (arrow) and almost continuous line of flaps (arrowhead); scale bar, 1 μm . (F) Valve with annulus (arrow) and adjacent sub-central pore (arrowhead); scale bar, 1 μm . (G) Internal view of a valve with the sub-central pore (arrowhead); scale bar 1 μm . (H and I) Nearly trapezoidal copulae of different length and shape; note the almost continuous hyaline ridge close to one border (arrowheads); scale bar, 1 μm .

Table S4). The flap-like processes at the margin of the valve face are generally blunt and denser (1.17–3.36 in 1 μm ; Fig. 2F) than in other species (Fig. 2F). The valve mantle is wide and slanting toward the valvocopula. This gives a markedly convex outline to the whole valve (Fig. 2, D, F), resulting in a pronounced constriction at the junction between sibling cells, which is also discernible in LM (Fig. 2C). The copulae are nearly trapezoidal (Fig. 2, I, J) or rarely ribbon-like (Fig. 2H), their width at times decreasing from the valve toward the mid of the girdle. A thin hyaline ridge runs parallel to the shorter sides of the band, at times only seen along the two oblique ones, delimiting one or a few parallel rows of areolae (Fig. 2, H–J; Table S4).

Crosswise oriented striae are present on the copulae at a density of 6–10 in 1 μm , becoming less regular and dense toward the hyaline ridge (Fig. 2J). Resting spore formation was not observed in nutrient depleted media. Cell enlargement was not directly observed either, although cell size did vary over the time in individual cultures.

Leptocylindrus danicus Cleve 1889 (Figs. 3, A–I; and 4, A and B)

Emended diagnosis: Cells 3–13 μm in diameter, 22–75 μm in perivalvar length, forming filamentous chains. Plastids numerous, lens-shaped or ellipsoidal. Valves with a distinct central annulus delimiting a group of poroid areolae. Sub-central pore adjacent to the annulus. Poroid areolae (18–30 in

1 μm) arranged in radiating striae (11–16 in 1 μm). Mantle evenly curving proximally and continuing almost perpendicular to the valve face distally. Copulae elongated and nearly trapezoidal, with areolae along irregular crosswise striae. Auxospore nearly spherical, smooth, covered with weakly silicified circular plates. Spores semi-globular, composed of two unequal valves bearing spines.

Holotype: figure on p. 54 in Cleve 1889

Isotype: Plate II, figure 4 in Cleve 1894

Epitype: Strain SZN-B650, Figure 3, A–I, collected on 15 June 2010 at the LTER-MC station in the GoN (40.80° N, 14.25° E). A permanent slide is deposited at the SZN Museum as slide no. SZN-B650-01.

Additional description: The filamentous chains are often composed of more than one hundred cells (≤ 165 , Table S3). The plastids are numerous (7–36), discoid or rarely ovoid (Fig. 3, A and B), and are regularly distributed across the perivalvar axis along the cell periphery. The valve faces have a slightly more silicified central area, with a group of areolae delimited by the central annulus (Fig. 3, F and G). The striae run from the annulus across the mantle and at times split into two half-way on the valve face (Fig. 3F). The sub-central pore is conspicuous (0.06–0.13 μm) with a hyaline margin which is also visible on the internal surface of the valve (Fig. 3G), and is generally located adjacent to the annulus (at least in 80% of the observed valves). A circle of spines or flap-like, triangular processes is found at the margin of the valve face (Fig. 3, C–E). The mantle bends proximally, and then runs almost perpendicular to the valve face toward the valvocopula (Fig. 3C). It is perforated by parallel striae of round areolae which almost always are in continuity with those of the valve face (Fig. 3, D and F). The girdle consists of nearly trapezoidal copulae, with irregular crosswise striae of poroid areolae. A thin hyaline ridge runs parallel to the margins of the two oblique sides of the copulae (Fig. 3, H and I), while one or more irregular hyaline ridges are seen at times along the shorter margin of the two parallel sides. Crosswise or obliquely oriented striae (10–15 in 1 μm) are present on the bands, becoming less regular toward the hyaline ridge (Fig. 3, H and I). Under nutrient-depleted conditions, spherical auxospores covered by siliceous scales (Fig. 4, A and B) are produced which turn into semi-globular spiny spores (Fig. 4B), 10.0–12.5 μm in diameter. Each spore is composed of two unequal valves, a bigger semi-circular epivalve (Fig. 4B) and a relatively smaller hypovalve (Fig. 4B). Both the epivalve and hypovalve have triangular or pyramidal spines, which have smooth, or at times, branched or serrated margins (Fig. 4B).

Leptocylindrus hargravesii Nanjappa and Zingone **sp. nov.** (Figs. 5, A–K; and 6, A and B)

Diagnosis: Cells 3–15 μm in diameter and 30–90 μm in perivalvar length, with heavily silicified

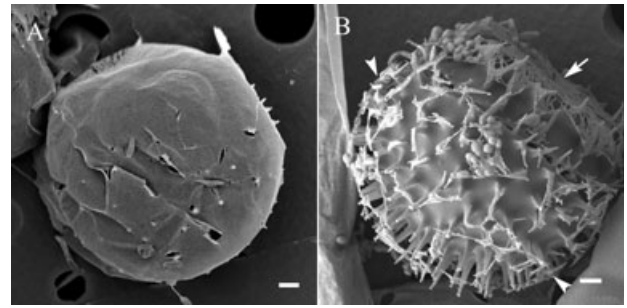


FIG. 4. Spore morphology of *Leptocylindrus danicus*, strain SZN-B650. SEM: A and B. (A) Auxospore in girdle view; scale bar, 1 μm . (B) Spore in girdle view; note the size of epivalve (arrowhead) and hypovalve (arrow); scale bar, 1 μm .

frustules, forming filamentous chains. Plastids numerous, lens-shaped to ellipsoidal. Valves with a hardly visible central annulus, delimiting a group of poroids. Sub-central pore generally not adjacent to the annulus. Poroid areolae (10–14 in 1 μm) arranged in radiating striae (6–11 in 1 μm), in most cases interrupted before reaching the mantle. Mantle evenly curved proximally, almost perpendicular to the valve face distally. Copulae elongated and nearly trapezoidal, with areolae along irregular crosswise rows. Auxospore nearly spherical, smooth, covered with weakly silicified circular plates. Spores semi-globular, composed of two unequal valves bearing spines.

Holotype: Strain SZN-B781, Figures 5, A–K; and 6, A and B, collected on January 25, 2011 at the LTER-MC station in the GoN (40.80° N, 14.25° E). A permanent slide has been deposited at the SZN Museum as slide no. SZN-B781-01.

Etymology: The species is dedicated to Paul Hargraves, who greatly contributed to the understanding of the diversity and life cycle of the genus *Leptocylindrus*.

Additional description: The cells have a relatively stout frustule (Fig. 5, A–C). In culture, filamentous chains may be composed of up to 162 cells (Table S3). Numerous (9–55) discoid or ellipsoidal plastids are regularly distributed along the cell periphery (Fig. 5, A and B). The striae radiating from the annulus are often interrupted distally, generally not reaching the mantle. The density and size of the areolae on the striae also tend to diminish toward the mantle (Table S4). The annulus (Fig. 5, G, H, J) is often hardly visible since the central part of the valve can be heavily silicified (Fig. 5E). A prominent pore (0.09–0.13 μm) is observed close to the annulus but never adjacent to it. It has a hyaline margin which is also seen on the internal surface of the valve (Fig. 5F). A variable position in cultured material is at times observed for this pore, which is occasionally found close to the valve face margin (Fig. 5, G, H, J). Marginal flap-like triangular structures are present along the border between mantle and valve face (Fig. 5C). The mantle is set

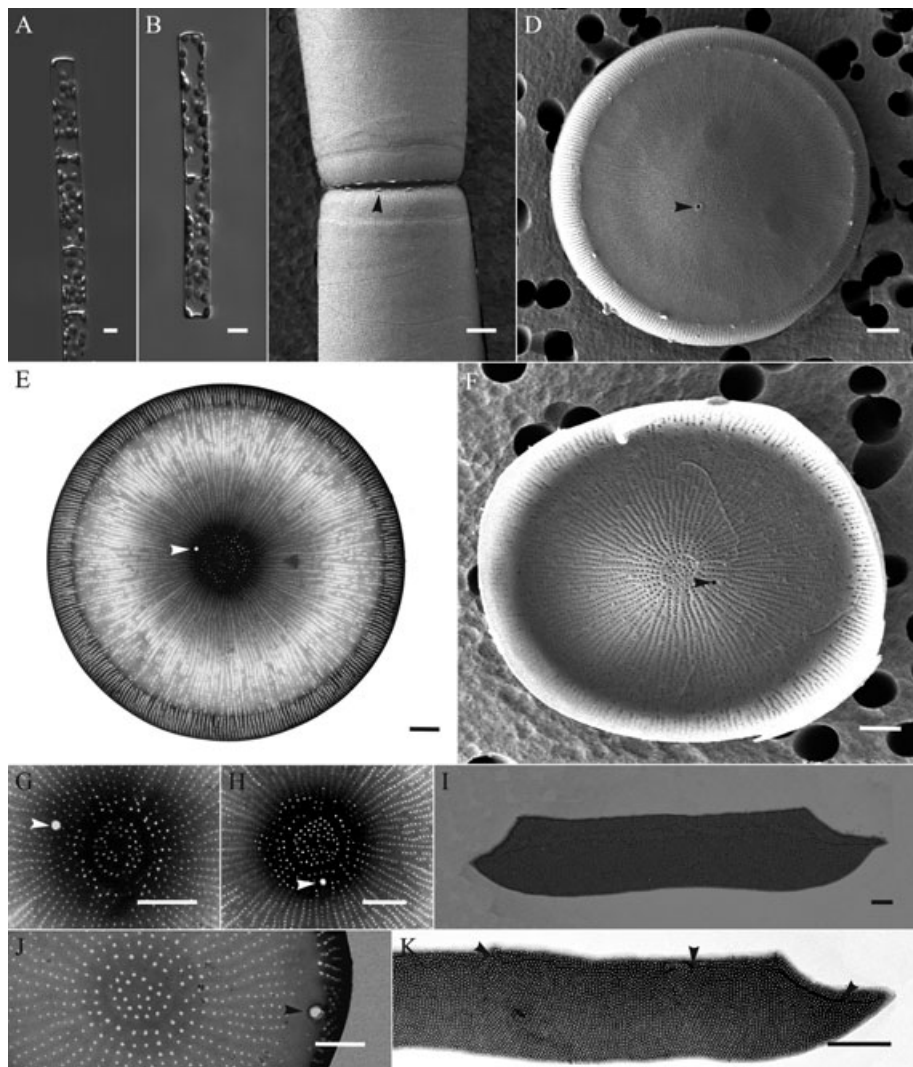


FIG. 5. *Leptocylindrus hargravesii*, strain SZN-B781. LM, DIC: A and B. SEM: C, D and F. TEM: E and G–K. (A) Colonial cells; scale bar, 5 μ m. (B) Chain of two cells showing the convex or concave valve surface and discoidal plastids; scale bar, 5 μ m. (C) Detail of two cells joined by the valve face, with flaps alternating along the marginal ring (arrowhead); scale bar, 1 μ m. (D) Valve with sub-central pore and hardly visible flaps; scale bar, 1 μ m. (E) Valve with sub-central pore (arrowhead); note the heavily silicified central area; scale bar, 1 μ m. (F) Internal view of a valve, with the sub-central pore (arrowhead); scale bar, 1 μ m. (G, H, and J) Details of valves, showing the variable position of the sub-central pore; scale bar, 1 μ m. (I and K) Heavily silicified, nearly trapezoidal copulae of different length and shape; note the almost continuous hyaline ridge close to one border (arrowheads); scale bar, 1 μ m.

off from the valve face at an angle of about 90°, proximally bending toward the valve face (Fig. 5, C and D). It has round to rectangular areolae arranged in parallel striae, which often are not continuous with those of the valve face. A thin hyaline ridge runs parallel to one margin of the trapezoidal copulae, generally opposite to their longer side, delimiting one or a few parallel rows of areolae (Fig 5, I and K). A hyaline ridge at times can be seen only along the oblique sides of the copula. Crosswise oriented striae are present on the copulae at a density of 8–12 in 1 μ m, becoming less regular toward the hyaline ridge (Fig. 5I). Spiny, semi globular spores (10.5–16.5 μ m in diameter) are formed upon induction by deprivation of nutrients (Fig. 6,

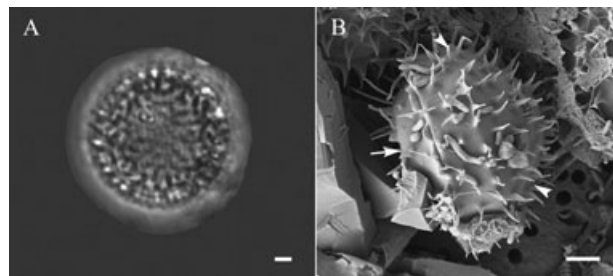


FIG. 6. Spore morphology of *Leptocylindrus hargravesii*, strain SZN-B781. LM, DIC: A; SEM: B. (A) Spiny spore; scale bar, 1 μ m. (B) Spore in girdle view; note the size of epivalve and hypovalve; scale bar, 1 μ m.

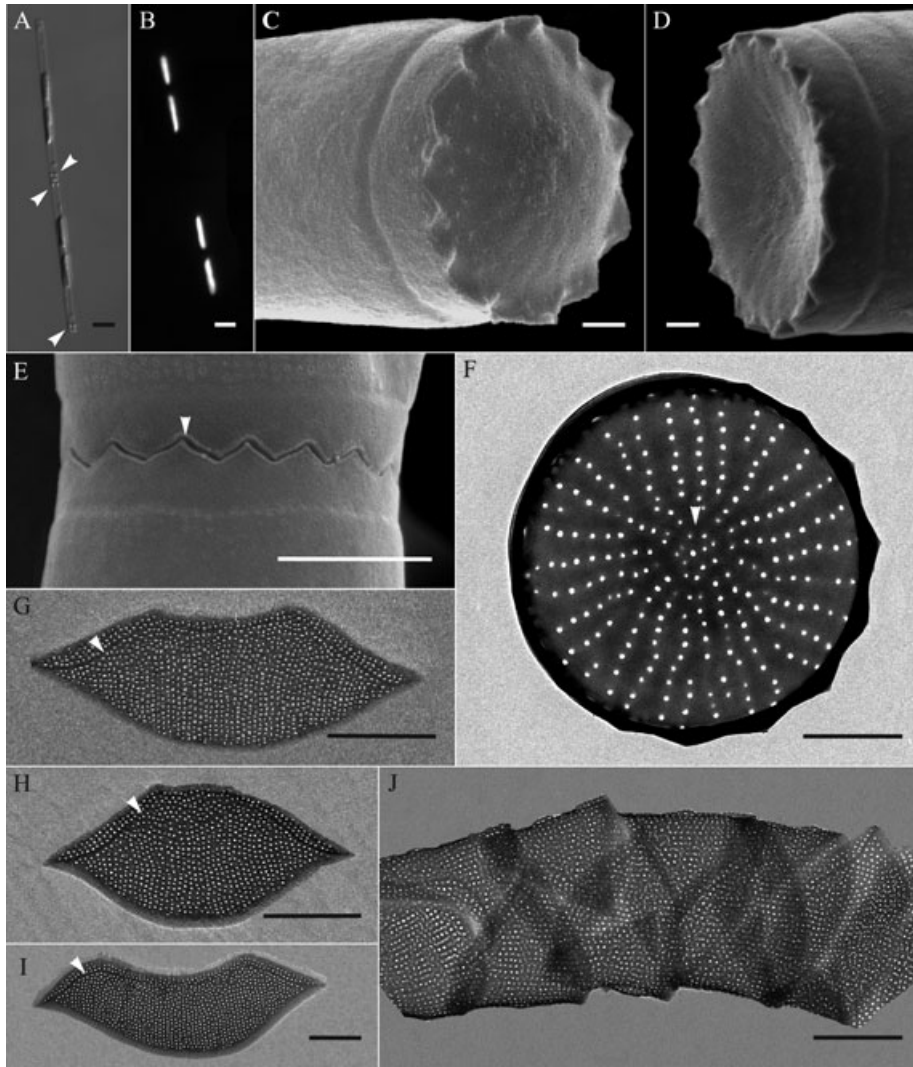


FIG. 7. *Tenuicylindrus belgicus*, strain SZN-B739. LM, DIC: A; epifluorescence: B. SEM: C, D and E. TEM: F–J. (A) Chain of two cells; note the elongated plastids and a couple of granules at both the cell ends (arrowheads); scale bar, 5 μ m. (B) Same chain as in A; note the shape of the plastids; scale bar, 5 μ m. (C) Valve with convex valve face and the crown-shaped mantle; scale bar, 0.2 μ m. (D) Valve with concave valve face; scale bar, 0.2 μ m. (E) Detail of the junction between two sibling cells; note the zig-saw fit (arrowhead) and the smooth, poreless mantle; scale bar, 1 μ m. (F) Valve ultrastructure; scale bar, 1 μ m. (G) Valvacopula; note the hyaline ridge close to the border (arrowhead); scale bar, 1 μ m. (H) Copula; note the hyaline ridge close to the border (arrowhead); scale bar, 1 μ m. (I) Copula with a less common shape; note the hyaline ridge close to the border (arrowhead); scale bar, 1 μ m. (J) Cell in girdle view; note the arrangement of the copulae; scale bar, 1 μ m.

A and B). These spores develop inside smooth auxospores, which show disc-like scales (data not shown). Each resting spore consists of two unequal sized valves, a larger epivalve and a smaller hypovalve (Fig. 6B). Both valves are heavily silicified and covered with pyramidal spines with smooth or at times serrated margins and residual scale fragments sticking to them (Fig. 6B).

***Tenuicylindrus* Nanjappa and Zingone gen. nov.**

Diagnosis: Cylindrical cells, joined by their valve faces to form filamentous chains. Valve face with an irregular central annulus and radial rows of pores. Valve mantle perpendicular to the valve face, with scarce pores. Distal edges of the valves and of the mantle forming triangular teeth which closely fit

those of the sister cells. Copulae are half bands with longitudinal rows of pores.

***Tenuicylindrus belgicus* Nanjappa and Zingone, comb. nov.** (Fig. 7, A–J)

Basionym: *Leptocylindrus belgicus* Meunier 1915, *Mémoires du Musée Royal D'Histoire Naturelle de Belgique, Hayez, Imprimeur de l'Académie Royale de Belgique Bruxelles*, 47, Plate XII, figure 4.

Diagnosis: Cylindrical cells, 2.0–2.5 μ m in diameter and 23.6–50.0 μ m in perivalvar length, forming filamentous chains, slightly undulating in culture material but general straight in nature. Two thin and elongated plastids per cells. Two granules visible at each end of the cells, under the valve face. Circular valves with radial striae (13–18 in 1 μ m) of pores.

Mantle perpendicular to the valve face, smooth and with scarce pores, proximally ending with a zig-zag margin joining the valve face rim. Triangular teeth-shaped processes at the boundary between mantle and valve faces, closely fitting those of the sister cells. Girdle composed of lip-shaped half-band copulae with longitudinal rows of pores. Spores not observed.

Holotype: Plate XII, figure 4 in Meunier (1915).

Epitype: Strain SZN-B739, Figure 7, A–J, collected on December 2, 2010 at the LTER-MC station in the GoN (40.80° N, 14.25° E). A permanent slide has been deposited at the SZN Museum as slide no. SZN-B739-01.

Etymology: The genus name refers to the extremely thin (*tenuis* in Latin) frustules of this species. The species epithet assigned by Meunier (1915) refers to the type locality of the species.

Additional description: Cells are thin cylinders with small and scarcely variable diameter and relatively long perivalvar axis (Fig. 7A, Table S3). In natural samples chains are always straight and comprised of two or three cells, whereas in culture they are often slightly curved or undulated and are comprised of many cells (2–14 cells per chain, Table S3). The frustule is delicate and only requires a weak acid treatment to eliminate the organic matter and preserve the morphological features. The two long and narrow leaf-like plastids are positioned on either sides of the nucleus along the girdle (Fig. 7, A and B). The valve face is either convex or concave (Fig. 7, C and D), the concave valves fitting the convex ones of the sister cell in the chains. The central area of the valve has a group of areolae that is delimited by a hyaline, at times ill defined, annulus. Over the valve face, round areolae of variable size are placed along radiating striae (Fig. 7F). The mantle is smooth, with sparse areolae, and lies perpendicular to the valve face plane. The margin toward the valvacopula is smooth, while a sharp, zigzag-edged margin is present on the other side, conferring the mantle a crown-like shape. The zigzag margin of one cell perfectly fits that of the adjacent cell, thus producing chains with no constrictions at the boundary between two sister cells (Fig. 7E). The copulae have pointed ends and often show a lip-like outline. They bear longitudinal, more or less regular, striae of areolae. One edge of the copula is smooth while the opposite one is finely serrated (Fig. 7I). Cultured cells maintain a rather constant cell size range, with no indication of vegetative cell enlargement or of auxospore formation. Spores were not observed under nutrient-deprived conditions.

Seasonal distribution: The seasonality for the five *Leptocylindraceae* in the GoN was reconstructed based on the time the 85 strains were brought in cultivation (Table S1). This was possible considering that isolation of *Leptocylindrus* and *Tenuicylindrus* strains was regularly (almost weekly) performed over more than 1 year. Additional information was obtained

through careful observations of the net samples collected on a weekly basis. *L. aporus* strains were all retrieved from mid-July to mid-November, whilst *L. convexus* strains were isolated from January to toward the end of March and also observed in April in net samples. Strains of *L. danicus* were retrieved from mid-November to mid-July, whilst *L. hargravesii* strains were only retrieved in December and January. Finally, *T. belgicus* strains were retrieved from the end of August to the beginning of November.

Molecular phylogenies. Overviews of the phylogenetic relationships among the sequences of *Leptocylindrus* and *Tenuicylindrus* species inferred from the six different molecular markers (nuclear SSU rDNA, nuclear LSU rDNA, 5.8S rDNA, plastid SSU rDNA, *rbcl* and *psbC*) are shown in Figure 8. Information about the alignment lengths and number of variable parsimony informative positions is presented in Table S5 in the Supporting Information. The summary of base substitutions inferred through the best-fit model for different regions is presented in Table S6 in the Supporting Information. Although these numbers varied among the markers, almost all contained sufficient information to distinguish the studied species. Minor intraspecific variation was present (Fig. 8), but sequences differed radically among strains of different species. Interspecific alignment of the ITS-1 and ITS-2 sequences was feasible only between *L. danicus* and *L. hargravesii*, showing base changes at least at 29 positions. Comparison of ITS-2 secondary structures of *L. danicus* and *L. hargravesii* revealed four HCBC's (Fig. 9). Among the alignments of the other markers, those of 5.8S rDNA and plastid SSU rDNA provided the lowest number of variable positions (33 and 34, respectively; Table S5) whereas the nuclear SSU rDNA alignment provided the highest number (358; Table S5). All the phylogenies inferred from these alignments (Fig. 8) showed essentially the same relationships, with *L. hargravesii* as sister to *L. danicus* and *L. aporus* as sister to *L. convexus*. *L. minimus* is shown only in the SSU-based tree because a single nuclear SSU rDNA sequence assigned to this species was recovered from GenBank.

Dissimilarities among *Leptocylindrus* species were generally much higher than those among species in other diatom genera, especially on the nuclear SSU and the nuclear LSU rDNA (Table S7 in the Supporting Information). The differences were especially pronounced between *Leptocylindrus* and *Tenuicylindrus* (SSU: 16%; LSU 24%). Dissimilarity values within the *Chaetoceros-Bacteriastrum* species (SSU: 9%; LSU: 19%) were closer to those of *Leptocylindrus* (SSU: 14%; LSU 18%) whereas those of *Pseudo-nitzschia-Fragilariopsis*, *Aulacoseira*, *Skeletonema* and *Sellaphora* were markedly smaller (SSU: <4%; LSU <10%).

In the analysis of the concatenated sequences of the nuclear SSU rDNA and the plastid encoded *rbcl* and *psbC* (Fig. 10 and Fig. S1 in the Supporting

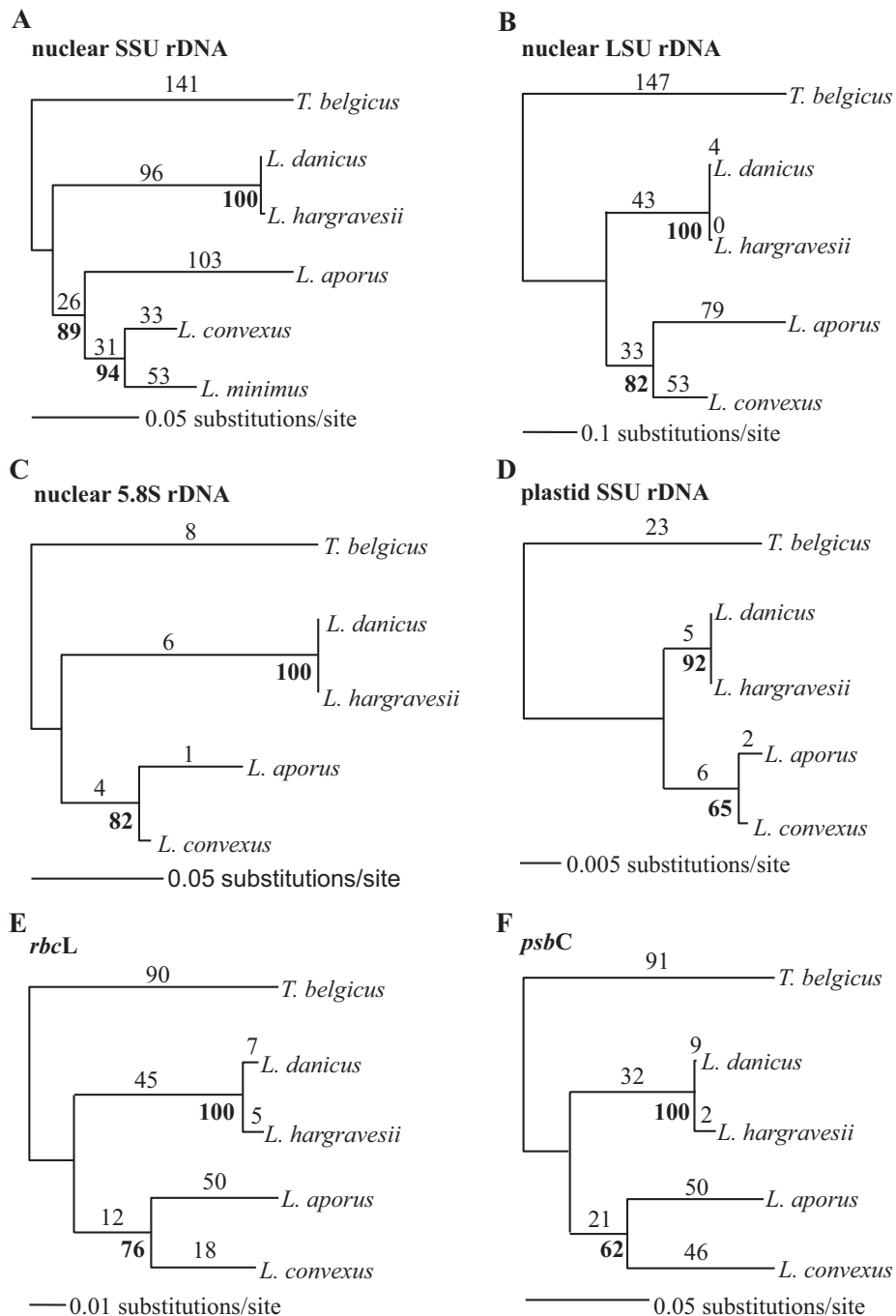


FIG. 8. Maximum likelihood relationships inferred for each of the alignments used in this study for *Tenuicylindrus* and *Leptocylindrus* species. Bootstrap values have been generated with 1,000 replicates and are indicated below the internodes. Numbers of synapomorphies resulting from maximum parsimony analysis of the data sets are indicated above each of the branches in each of the trees.

Information), *Tenuicylindrus* was resolved as sister to monophyletic *Leptocylindrus* and species of the latter genus showed the same relationships among them as those shown by the analysis of individual markers (Fig. 8). *Corethron hystrix* was resolved as sister to Leptocylindraceae in the basal clade of the diatom tree. The remainder of the radial centric diatoms included in this alignment resolved into two clades

making the radial centrics paraphyletic. Bi- and multipolar centrics (including secondarily radial centric Thalassiosirales) grouped in a clade, except for *Attheya*, which was resolved with high bootstrap support as sister to the pennates.

A RAxML-tree of the nuclear SSU rDNA (Fig. S2 in the Supporting Information) resolved relationships among species in *Leptocylindrus* and *Tenuicylindrus*

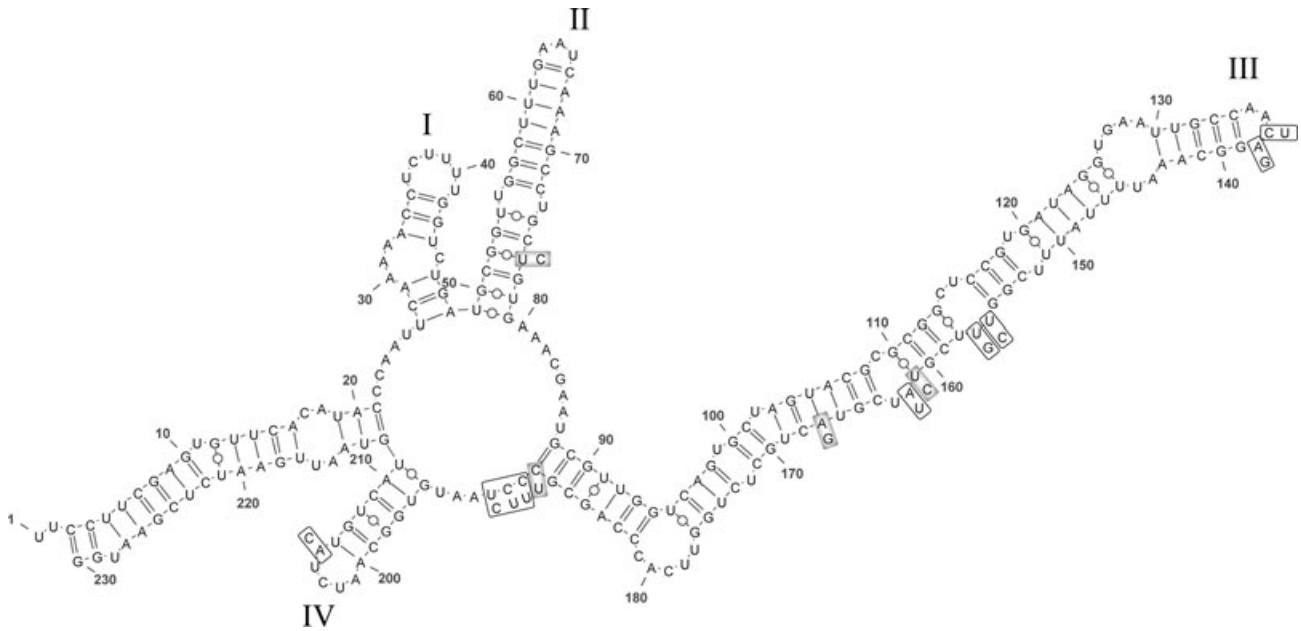


FIG. 9. Secondary structure of the nuclear ITS2 rDNA of the species *Leptocylindrus hargravesii* and *L. danicus*. The secondary structure was based on *L. hargravesii* CCMP1856 sequence and base changes for *L. danicus* are marked. HCBCs are highlighted while non-CBCs are simply marked. The four stems are numbered with roman numerals.

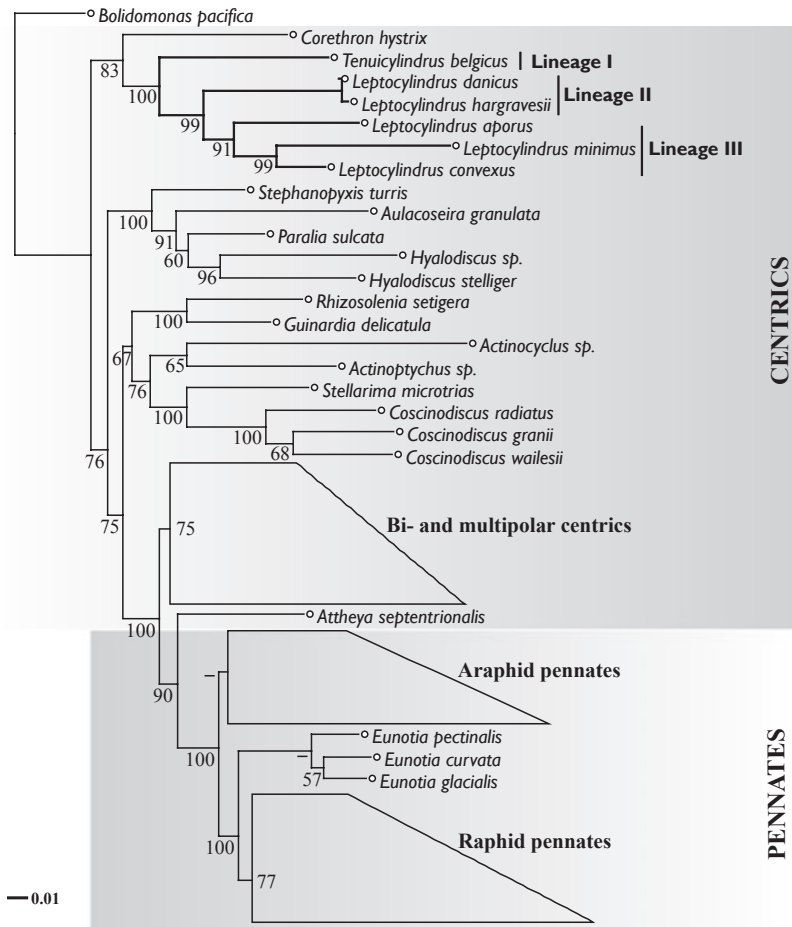


FIG. 10. Maximum likelihood tree inferred from concatenated SSU rDNA-*rbcL-psbC* sequences illustrating the relationship among *Tenuicylindrus*, *Leptocylindrus* species and other groups. Bootstrap values have been generated with 1,000 replicates.

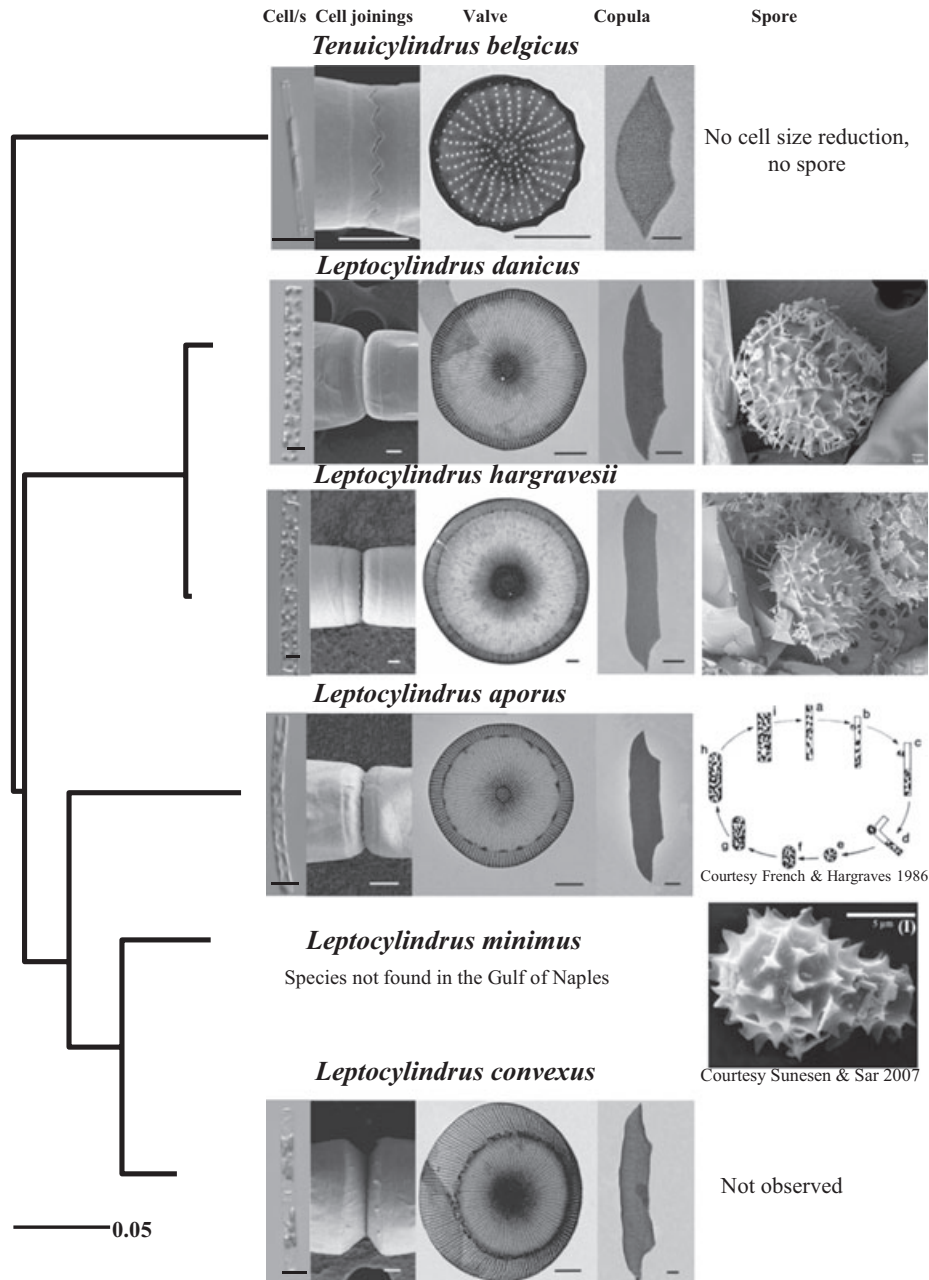


FIG. 11. Differential characters for *Leptocylinndrus* and *Tenuicylinndrus* species plotted on the SSU rDNA maximum likelihood tree. Scale bar, LM: 10 μ m, EM: 1 μ m.

as in the concatenated tree (Fig. 10 and Fig. S1), but showed only Leptocylinndraceae as the diatom basal clade. *Corethron hystrix* was shown in one of the two other radial centric clades, but together, radial centrics were paraphyletic. Relationships among bi- and multipolar centrics and pennates were resolved as in the tree inferred from the concatenated sequences with similar support values. A RAxML-tree of the *rbcL* resolved relationships among species in *Leptocylinndrus* and *Tenuicylinndrus* as in Figure 10 and recovered Leptocylinndraceae as basal clade, though with weak bootstrap support (Fig. S3 in the

Supporting Information). However, relationships among radial centrics, bi- and multipolar centrics and pennates were not resolved because bootstrap support for basal ramifications was low or lacking altogether. The *psbC* tree lacked any support for the basal ramifications and even left the relationships between *Tenuicylinndrus* and *Leptocylinndrus* and within the latter genus unresolved (Figure S4 in the Supporting Information).

The nuclear SSU rDNA tree topology among the *Leptocylinndrus* species and *Tenuicylinndrus* has been redrawn in Figure 11. Overall cell morphology, the

TABLE 1. Main distinctive morphological characters in *Leptocylindrus* and *Tenuicylindrus* species.

	<i>L. aporus</i>	<i>L. convexus</i>	<i>L. danicus</i>	<i>L. hargravesii</i>	<i>L. minimus</i>	<i>L. minimus</i>	<i>T. belgicus</i>
Source	Current study & French and Hargraves 1986	Current study	Current study	Current study	Hargraves 1990	Rivera et al. 2002	Current study
Cell diameter (μm)	3.5–10.6	3.0–8.0	3.0–13.0	3.0–15.0	1.5–4.5	2.0–5.2	2.0–2.5
Cell length (μm)	12.5–33.0	22.0–65.0	22.0–75.0	30.0–90.0	–	–	23.6–50.0
Plastid no.	3–13	3–11	7–36	9–55	1–2	1–2	2
Plastid shape	Discoid, ovoid	Ovoid, elongated	Discoid	Discoid	Elongated	Elongated	Elongated
Cells per chain	2–24	2–68	2–165	2–162	–	–	2–14
Valve to mantle ratio	2.9–8.4	2.4–4.0	5.6–11.5	5.3–14.3	–	–	–
Striae (in 1 μm)	9–13	6–10	8–13	7–11	13–18	8–13	7–11
Valve areolae (in 1 μm)	10–14	10–14	18–30	10–14	–	–	12–22
Constriction at the cell junction	Small	Marked	Small	Small	Small	–	Absent
Auxospores and resting spores	Not observed	Not observed	Spiny, semiglobular	Spiny, semiglobular	Spiny, globular with a neck	Not described	Not observed
Sub-central pore	Absent	Absent	Adjacent to annulus	Slightly away from annulus	Absent	Absent	Absent

link between sister cells, the ultrastructure of the valve face, copula and resting spore (Table 1) have been illustrated on the end-nodes of the tree for easy taxonomic identification.

DISCUSSION

The results of our study on morphological, molecular and life cycle characteristics of a series of strains belonging to the genus *Leptocylindrus* has shown that the species *L. danicus* consists of at least four distinct species. One of these, *L. aporus*, was described as a variety of *L. danicus*, while two others, *L. hargravesii* and *L. convexus* are new to science. A fifth species, so far identified as *L. minimus* in the area, fits the description of *L. belgicus*, but its profound ultrastructural and molecular differences from both *L. minimus* and all the other known *Leptocylindrus* species prompted the establishment of a new genus, *Tenuicylindrus*, to accommodate it.

The morphological similarities among the *Leptocylindrus* species in combination with the considerable nucleotide differences among them contrast with far smaller nucleotide differences among species within morphologically arguably more diverse diatom genera. One explanation is that the genus *Leptocylindrus* is an ancient one containing just a few genetically distinct remnant species whereas alternatively the marker regions of the *Leptocylindrus* species could evolve particularly fast. The resolution of *Tenuicylindrus* and *Leptocylindrus* in a basal clade in the nuclear SSU rDNA and rbcL trees as well as in the tree of concatenated sequences suggests that

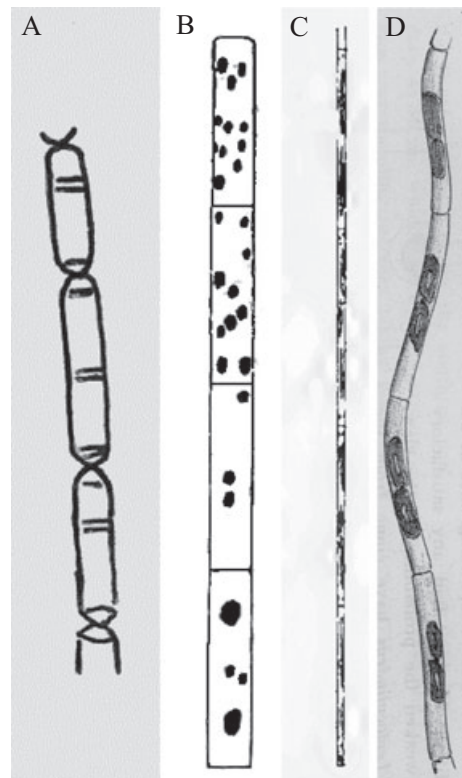


FIG. 12. Pencil diagrams of the species studied. (A) *Leptocylindrus danicus* redrawn from Cleve (1889). (B) *Leptocylindrus danicus* redrawn from Cleve (1894). (C) *Tenuicylindrus belgicus* redrawn from Meunier (1915). (D) *Leptocylindrus minimus* redrawn from Gran (1915).

these genera are ancient. Whether the species diversity is low or not remains to be tested by exploring species diversity in other regions by making use of, for instance, next generation sequencing approaches in combination with morphological approaches in plankton diversity.

Taxonomy. The taxonomic history of both genera, *Leptocylindrus* and *Tenuicylindrus*, i.e., of their type species, *L. danicus* and *T. belgicus*, is complicated, which affects to some extent the present definition of the two taxa and requires some arbitrary choices in the amendment of their descriptions. The taxonomy of *L. danicus* starts with the misrepresentation of the frustule shape by Cleve (1889) based on material collected in his expedition to the Kattegat area (Fig. 12A). Cleve drew the valves as convex, only contacting the next ones with a small surface or a point. Such features do not apply to any of the currently known species in *Leptocylindrus* or *Tenuicylindrus*. In addition, and in contrast with the protologue, the drawing showed some lines in the cingulum, which suggests that the band margins were at times visible. A few years later, Cleve (1894) stated that the species was “originally described from burnt and somewhat misshaped specimens” and provided a new illustration (Fig. 12B) and the following re-description: “cells cylindrical, with flat (dried convex) ends, forming filaments. Valves without processes or perceptible structure. – Connecting zone very thin, without annuli – Cell contents: a few scattered granular chromatophores. Diameter of the filament 0.01 mm. Length of the cell 0.03–0.06 mm”. The concept of *L. danicus* was reinforced by Gran (1915), who undertook a study in the Kattegat and described spiny, semi-circular resting spores produced through auxosporulation. These peculiar features for *L. danicus* spores were confirmed by a more recent study French and Hargraves (1986), which also reported the presence of a sub-central pore in the valve. Therefore, despite the initial uncertainty arising from a type material not representing the species correctly, there are several elements that concur to define the species *L. danicus* in modern terms.

The present finding of two genetically distinct groups of strains sharing most of the features used for the definition of *L. danicus* poses further problems as to (i) whether to separate them as distinct species or not, and (ii) which of the two is *L. danicus*. One possibility is to consider a single species, *L. danicus*, as a genetically diverse taxon. However, the genetic differences between the two groups of strains on all of the molecular markers (2 on SSU, ≥ 4 on LSU, ≥ 29 on ITS, ≥ 12 on *rbcL* and ≥ 11 on *psbC*), combined with the subtle, but consistent, morphological differences between these two groups of strains, support the hypothesis that these groups belong to different species. Four HCBC's, and no CBC's, were found in the ITS-2 secondary structure between *L. danicus* and *L. hargravesii*. The absence

of CBC's could be interpreted as lack of evidence for reproductive isolation. However, although the existence of CBCs in ITS-2 has been shown to correlate with reproductive isolation, no causal relationship exists between CBC's and reproductive isolation (Alverson 2008).

The decision about which of the two groups deserves the name and the designation of the neotype of *L. danicus* was arbitrary, though. Attempts were made to retrieve the type material, or material collected in the same cruise by Cleve, in the Swedish Museum of Natural History and Diatom Herbarium, The Academy of Natural Sciences, Philadelphia, USA as well as at the National Botanical Garden of Belgium, where Cleve's materials are kept, but these efforts failed. The final choice was hence made based on the higher number of strains isolated in the study area for one of the two genotypes, which was considered *L. danicus*. The neotype strain of *L. danicus* was also selected for further physiological, metabolomics and transcriptomic analyses, presently in progress (Nanjappa 2012). The other genotype, successfully isolated only three times, was hence described as a species new to science, *L. hargravesii*.

The designation of the new combination of *L. aporus* based on the description of *L. danicus* var. *apora* is supported by morphological and life cycle characteristics discussed in the next section as well as by the presence in GenBank of one nuclear SSU rDNA sequence obtained from a strain apparently used by (French and Hargraves 1986) in the description of the variety (Linda K. Medlin, personal communication), which is identical to the corresponding sequence of the material examined in the present study.

The establishment of the new genus *Tenuicylindrus*, which presently includes a single species *T. belgicus*, is mainly based on its unique ultrastructural features, which differ markedly from those shared among all of the presently known *Leptocylindrus* species. The differences observed in the valve structure and cell junction between *T. belgicus* and *Leptocylindrus* species are particularly relevant in the light of the remarkable morphological stasis in the Leptocylindraceae. By contrast, the inclusion of *T. belgicus* in the genus *Leptocylindrus* would only be supported by the overall resemblance of cell and chain shape. Moreover, phylogenies inferred from nuclear SSU rDNA and *rbcL* sequences show that *T. belgicus* is sister to the clade including all the species of *Leptocylindrus*, while the *psbC* tree resolves *Tenuicylindrus* away from the clade of *Leptocylindrus* (although sister relationships are not falsified given insufficient bootstrap support). Despite the limited information presented in the original description of the designed type species *T. belgicus* (basionym *L. belgicus*, Meunier 1915, Fig. 12C), its resemblance with the material examined from the GoN is striking (Fig. 7), particularly in the presence of the sub-valvar granuli which are typi-

cal of the material from the GoN and also perceivable in the illustration by Meunier (1915).

Morphological and life cycle features of Tenuicylindrus and Leptocylinndrus species. Leptocylinndraceae arguably possess one of the simplest known diatom ultrastructures, and until now they were considered to comprise *L. danicus* and *L. minimus*, in addition to the debatable taxon *L. mediterraneus*. Vegetative cells of *L. danicus* and *L. minimus* are morphologically similar, the main distinction between them being the cell size, plastid number and shape, and spore morphology. The type material of *L. minimus* (Fig. 12D) shows undulating cell chains (Gran 1915), but this feature does not seem to be confirmed in the literature (Hargraves 1990), nor unique to this species based on our observation in cultured material. The results of the morphological and phylogenetic analyses in the present study suggest instead the existence of at least six taxa in the family Leptocylinndraceae; these can be arranged into three main morphological groups, which correspond to three lineages (I to III) identified in the phylogenetic tree (Fig. 10). These groups are distinct from each other for morphological and life cycle features, whereas morphological differences within the groups are generally subtle.

The species *T. belgicus* (Lineage I) is markedly different from all other known *Leptocylinndrus* species (Fig. 12). Like *L. minimus*, *T. belgicus* possesses two elongated plastids and is thin, but has a narrower size range (2–2.5 µm; Meunier 1915 and this study), as compared to *L. minimus* (1.5–5.2 µm; Hargraves 1990, Rivera et al. 2002). In addition, the two granules under each valve in *T. belgicus* provide an alternative means to discriminate the species in LM. With respect to valve and girdle band ultrastructure, *T. belgicus* is different from any *Leptocylinndrus* species. The valve mantle of *T. belgicus* is perpendicular to the valve face, while in all *Leptocylinndrus* species it lies proximally in the same plane with the valve face, marginally bending and becoming perpendicular to it. The mantle of *T. belgicus* has one free margin with a zig-saw outline, connecting to the mantle of the sibling cell, and the opposite margin is attached to the valvacopula, whilst in *Leptocylinndrus* both mantle margins are smooth and attached to the valve face and valvacopula, respectively. Short interlinking, triangular processes, involved in the tight association between neighboring cells, have been documented in several fossil radial centric species (Gersonde and Harwood 1990) and can be considered an ancestral mode of chain formation (Crawford and Sims 2008). In addition, the mantle in *T. belgicus* does not show the striae and areolae that are found in *Leptocylinndrus*. Finally, the intercalary bands in *T. belgicus* often have a lip-like outline with pointed ends, while in *Leptocylinndrus* they are nearly trapezoidal or collar-like. All these differences in several features that are instead rather homogenous across *Leptocylinndrus* species support the establishment of a new genus, *Tenuicylinndrus*,

which is also supported by the large nucleotide-differences. Another peculiarity of *T. belgicus* is that it maintains a constant cell size throughout the life cycle, with no clear signs of vegetative cell enlargement. Constant cell size has also been observed in some other diatoms including, for instance, *Phaeodactylum tricornutum* (De Martino et al. 2007).

The next two lineages are assigned to the monophyletic genus *Leptocylinndrus*. The two members of Lineage II, *L. danicus* and *L. hargravesii*, have both a sub-central pore, which in *L. danicus* is adjacent to the hyaline ridge in 80% of cells in healthy cultures, whilst in *L. hargravesii*, it is never observed adjacent to the hyaline ring. This difference may however be difficult to appreciate in old cultures of both species, where the pore position on the valve at times varies. Morphometric characteristics also differ between the two species. The striae and areolae density on the valve face and the striae density on the mantle are higher in *L. danicus* than in *L. hargravesii*, with scarce or no overlap in the ranges between the two species. The valve striae often interrupt before reaching the mantle in *L. hargravesii*, while they continue all over the valve and across the mantle in *L. danicus*. The annulus is larger in *L. hargravesii*, while the center of the valve appears more densely silicified. Indeed *L. hargravesii* strains appear to be considerably more silicified and stouter than *L. danicus* and, accordingly, the samples of the former prepared for SEM retain their morphology better than the latter. In LM, the above-mentioned differences are hardly appreciable, but *L. hargravesii* generally has a larger perivalvar axis and a higher number of plastids than *L. danicus*. However, the number of plastids per unit of cell volume is similar in the two species.

In both *L. danicus* and *L. hargravesii* sexual reproduction was readily induced in monoclonal cultures, producing similar types of auxospores and spores. In all other diatom genera the auxospore produces a vegetative cell of the maximum size (see Montresor and Lewis 2006 for a review). The spores produced in *L. danicus* and *L. hargravesii* were similar, and in both cases they varied in size, probably depending on the parent cell size.

Lineage III includes three species without the sub-central pore, *L. aporus*, *L. minimus* and *L. convexus*. In the light microscope *L. aporus*, the outermost taxon within the lineage, can be differentiated from other species observed in this study based on the relatively smaller size and the number and shape of the plastids, which are ovoidal as compared to lenticular in *L. danicus* and *L. hargravesii*, more elongated in *L. convexus* and elongated in *L. minimus*, and are generally more than two as compared to the latter species (Table 1). Morphological analysis of *L. minimus* was limited to literature data (Hargraves 1990, Rivera et al. 2002) as no isolate from the GoN matched this species. Apart from striae density on the valve (Table 1), *L. aporus* and *L. minimus* are rather similar

in valve ultrastructure, but could be distinguishable based on size range and number and shape of plastids, although we have limited experience of intraspecific variability of these characters in natural populations. As a matter of fact, during summer, when the most abundant *Leptocylindrus* species in the GoN is *L. aporus*, we often observe thin and somewhat spoiled cells with 1–3 plastids which would be hardly distinguished from *L. minimus*, were the latter species also present in the area. In contrast, the wide mantle and the markedly convex valves resulting in a constriction at the cell junction are quite distinctive for *L. convexus* in comparison with other *Leptocylindrus* species within and outside Lineage III. In addition, *L. convexus* is generally larger than *L. aporus* and *L. minimus* and the plastids, elongated and often arranged in four around the nucleus, are also peculiar to this species, which has been lately identified in LM in the natural material from the GoN in several cases.

Sexual reproduction and spore formation were not observed in the species of lineage III, at least under the same conditions that stimulated these processes in the two species of Lineage II. Vegetative cell enlargement through auxospore-like structures was observed in *L. aporus*, in agreement with the observations of (French and Hargraves 1986). A vegetative cell enlargement was first reported by von Stosch (1965) in *Achnanthes longipes*, *Ditylum brightwellii* and *Biddulphia pulchella*, followed by similar observations on a number of centric diatoms, for example, *Skeletonema costatum* (Gallagher 1983), *Coscinodiscus wailesii* (Nagai et al. 1995), as well as the pennate diatom *Achnanthes longipes* (Chepurnov and Mann 1999). The vegetative cell enlargement is believed to have a selective advantage because of the lower energy requirement as compared to sex, and because it overcomes the risk of finding a mate of the opposite mating type. *L. minimus* is reported to produce spiny globular spores with a neck shaped structure at the basis (Hargraves 1990), clearly differing from the vegetative cells, but whether they also develop from a sexual auxospore is unclear. This unique derived feature, along with the number and shape of the plastids, could also help discriminating this species from *L. aporus*, which instead does not form spores. Spores were not produced in *L. convexus* cultures either, but size changes were observed regularly like for *L. aporus*.

In LM, it is relatively easy to distinguish the cultures of the five species examined, but in natural samples this is not as straightforward due to at times sub-optimal conditions of the cells in the natural environment and to a lack of information on the intraspecific variability of the different characters. For instance, it is often impossible to discriminate among *L. danicus*, *L. hargravesii* and *L. aporus*, in case plastid shape is not well preserved. In such cases electron microscopic examination may permit identification, but in some

cases confirmation from molecular analyses may be required.

Spatial and temporal distribution of the species. *Leptocylindrus* species have been considered widespread, mostly coastal, with numerous records of their occurrence and often being a major contributor of the diatom bloom. *T. belgicus* has never been reported elsewhere after its first report by Meunier (1915) from the Belgian coast. However, this may be due to a lack of recognition of this taxon as a species different from *L. minimus*. Indeed, the species illustrated in Round et al. (1990, 342, figure a) as *L. danicus* clearly shows the characteristic features that are identified in *T. belgicus*. Unfortunately, it is not possible to determine the geographic origin of the specimen illustrated in that picture. Other specimens attributable to *T. belgicus* are illustrated by Kraberg et al. (2010, page 82, figures a and b) from the North Sea. Interestingly a specimen of *T. belgicus* illustrated in TEM is also reported in the website Microflora/fauna of Yokohama (University of Yokohama 2012), which demonstrate the presence of the species along the west Pacific coasts of Japan. The actual *L. minimus*, with illustrations showing distinctive features of either vegetative cells or spores, is presently reported from Northern Europe (Kraberg et al. 2010), Narragansett Bay (Hargraves 1990) and Argentinian waters (Sunesen and Sar 2007). Interestingly, Sunesen and Sar (2007) also report the presence in Argentinian waters of specimens that match *L. hargravesii* both in the position of the sub-central pore and in the density of pores and striae in the valve. The distribution of the latter species appears to overlap that of *L. danicus* not only in the GoN (this study), but also in Narragansett Bay, since some valves shown in French and Hargraves (1986), e.g., figure 6, E and M, show the sub-central pore quite distant from the annulus, whereas others, e.g., figure 6, A, C, show it close to the annulus. Specimens of *L. minimus* from Chilean waters (Rivera et al. 2002) are described with 1–2 plastids, but with a striae density of 8–13 in 1 μm , which matches *L. aporus* rather than *L. minimus* features (Table 1). Considering that narrow *L. aporus* specimens with one or two plastids are commonly observed in the GoN in summer, the material from Chilean waters could in fact belong to *L. aporus*. In this case, the presence or absence of resting spores, or molecular data, would be essential to confirm the species identification.

The species examined in this study are present in the study area with different cell densities and seem to have different seasonal patterns. Although broadly qualitative and subject to problems related to cell viability under laboratory conditions, the available information indicates that *L. danicus* has a wider distribution in time as compared to other species, spanning from late autumn through mid-summer. In contrast, *L. hargravesii* and *L. convexus* showed the narrowest temporal distribution, namely only in the winter months, and they were rarely brought into

culture, indicating either an actual rarity in natural populations or a difficulty to grow under laboratory conditions. *L. aporus* is apparently the species responsible for the remarkable summer blooms in the GoN, so far attributed to *L. danicus*, and it is also found in autumn, along with *T. belgicus*. The latter species, which is the only one identified and enumerated in LM in the GoN as *L. minimus*, is recurrently found from late summer through the autumn (Ribera d'Alcalà et al. 2004), whereas Meunier (1915) and Kraberg et al. (2010) reported an early spring-summer period of occurrence. *L. minimus* was not found in the GoN, but the possibility that it escaped sampling cannot be totally excluded.

CONCLUSIONS

Based on our results, the diversity of the Leptocylindraceae has increased from 2 (or 3, including *L. mediterraneus*) to 6 (or 7) species, all of them quite distinct from the molecular point of view. To account for the observed molecular distances among taxa, the original range of taxonomic characters used for *Leptocylindrus* species, i.e., cell size and variable plastid number and shape, has been widened in our study by the addition of the presence and the position of the central pore, the shape of the valves and the valve mantle, and ultrastructural features of striae density and valve to mantle ratio. Yet these characters often require EM to be appreciated. Knowledge of the distribution of these species might benefit from application of sequence-based techniques including Fluorescent In Situ Hybridization (FISH), quantitative-PCR (qPCR) or construction of clone libraries with species-specific primers.

The increase in species number in Leptocylindraceae upon an in-depth-examination is comparable to cases of other diatoms such as *S. costatum* (Sarno et al. 2005, Sarno et al. 2007 Kooistra et al. 2008, Zingone et al. 2005), *Pseudo-nitzschia* (Lundholm et al. 2012 and literature therein) and *Chaetoceros* (Rines and Hargraves 1990, Kooistra et al. 2010). However, the similarities stop here. While species in the genera *Skeletonema* and *Pseudo-nitzschia* are closely related among one another, apparently diversifying rapidly, in the Leptocylindraceae the taxa are far more distantly related, even when the slowly evolving markers are taken into the account. The species in the Chaetocerotaceae are often somewhat more distantly related, but they show major morphological differentiation, while Leptocylindraceae have retained simple morphological and ultrastructural features which are basically shared among most of the species. In contrast to this apparent morphological stasis, *Tenuicylindrus* and *Leptocylindrus* species appear to have acquired (or retained) a variety of life cycle mechanisms, at times distinct from those observed in most other diatoms, encompassing little or no cell size reduction along the vegetative cycle, vegetative cell enlargement, spore

formation without apparent sexual mechanisms, and spore formation following sexual reproduction. Whether the differences in the life cycle mechanisms influence the success of the species and the extent to which these complex mechanisms have helped the species in the adaptation to their environment need to be studied.

Despite the high abundance and frequency over the year, the number of species uncovered in the Leptocylindraceae in the study area is far lower than in *Pseudo-nitzschia* and *Chaetoceros*, indicating a relative poorness of species for this genus. Considering that *Leptocylindrus* and *Tenuicylindrus* constitute the sister clade of a clade with all other diatoms, even the discovery of a series of additional species in these two genera would leave the clade as a species poor group in comparison to the estimated 100,000 species (Mann and Droop 1996) in the rest of the diatoms. Nonetheless, the true biodiversity in *Leptocylindrus* can only be uncovered by means of a thorough study on the global diversity of the genus.

The five species identified in this study are found in the GoN in distinct or partially overlapping periods, suggesting that they do have different ecological characteristics. Parallel investigations on these species indeed reveal that taxonomic differences are reflected in species-specific physiological properties, i.e., response to temperature and metabolite composition (Nanjappa 2012). Like in other cases (Kooistra et al. 2008, Degerlund et al. 2012, Huseby et al. 2012), these findings point at the functional diversity of morphologically similar species and emphasize the advantages of a better taxonomic resolution in the study of the ecology and diversity patterns of marine microbes.

The authors thank David G. Mann for his invaluable advices in the course of this investigation, M.V. Ruggiero for the troubleshooting with sequencing, E. Biffali and staff of Molecular Biology Service for sequencing services, F. Iammuno and G. Forlani for assistance with EM, R. Piredda for suggestions on the use of phylogenetic software and the MECA service for plankton sampling. Two anonymous reviewers are acknowledged for useful suggestions which improved the quality of the manuscript. D. Nanjappa and the whole investigation were supported by the SZN-Open University PhD program.

- Alverson, A. J. 2008. Molecular systematics and the diatom species. *Protist* 159:339–53.
- Alverson, A. J., Jansen, R. K. & Theriot, E. C. 2007. Bridging the Rubicon: phylogenetic analysis reveals repeated colonizations of marine and fresh waters by thalassiosiroid diatoms. *Mol. Phylogenet. Evol.* 45:193–210.
- Beszteri, B., John, U. & Medlin, L. K. 2007. An assessment of cryptic genetic diversity within the *Cyclotella meneghiniana* species complex (Bacillariophyta) based on nuclear and plastid genes, and amplified fragment length polymorphisms. *Eur. J. Phycol.* 42:47–60.
- Chepurnov, V. A. & Mann, D. G. 1999. Variation in the sexual behaviour of *Achnanthes longipes* (Bacillariophyta). II. Inbred monoecious lineages. *Eur. J. Phycol.* 34:1–11.
- Cleve, P. T. 1889. Pelagisk diatomeer fran Kattegat. In Petersen, C. G. J. [Ed.] *Det evidenskabelige udbytte af kanonbaaden*

- "Hauchs" togter i de Danske have indefor Skagen, I. Aarene. Andr. Fred. Høst & Sons Forlag., Copenhagen, pp. 53–6.
- Cleve, P. T. 1894. Redogørelse for de Sevnska hydrografiska undersökningarne åren 1893–1894. In Ekman, G., Pettersson, O. & Wijkander, A. [Eds.] *II. Planktonundersökningarna*. P. A. Nordstedt & Söner, Stockholm, pp. 1–16.
- Crawford, R. M. & Sims, P. A. 2008. Some principles of chain formation as evidenced by the early fossil record. *Nova Hedwigia Beih.* 133:171–6.
- Davis, C. O., Hollibaugh, J. T., Seibert, D. L. R., Thomas, W. H. & Harrison, P. J. 1980. Formation of resting spores by *Leptocylindrus danicus* (Bacillariophyceae) in a controlled experimental ecosystem. *J. Phycol.* 16:296–302.
- De Martino, A., Meichenin, A., Shi, J., Pan, K. & Bowler, C. 2007. Genetic and phenotypic characterization of *Phaeodactylum tricoratum* (Bacillariophyceae) accessions. *J. Phycol.* 43:992–1009.
- Degerlund, M., Huseby, S., Zingone, A., Sarno, D. & Landfald, B. 2012. Functional diversity in cryptic species of *Chaetoceros socialis* Lauder (Bacillariophyceae). *J. Plankton Res.* 34:416–31.
- Edgar, S. M. & Theriot, E. C. 2004. Phylogeny of *Aulacoseira* (Bacillariophyta) based on molecules and morphology. *J. Phycol.* 40:772–88.
- Evans, K. M., Wortley, A. H., Simpson, G. E., Chepurnov, V. A. & Mann, D. G. 2008. A molecular systematic approach to explore diversity within the *Sellaphora pupula* species complex (Bacillariophyta). *J. Phycol.* 44:215–31.
- French, F. & Hargraves, P. E. 1980. Physiological characteristics of plankton diatom resting spores. *Mar. Biol. Lett.* 1:185–95.
- French, F. W., III & Hargraves, P. E. 1985. Spore formation in the life cycles of the diatoms *Chaetoceros diadema* and *Leptocylindrus danicus*. *J. Phycol.* 21:477–83.
- French, F. W., III & Hargraves, P. E. 1986. Population dynamics of the spore-forming diatom *Leptocylindrus danicus* in Narragansett Bay, Rhode Island. *J. Phycol.* 22:411–20.
- Gallagher, J. C. 1983. Cell enlargement in *Skeletonema costatum* (Bacillariophyceae). *J. Phycol.* 19:539–42.
- Gersonde, R. & Harwood, D. M. 1990. Lower Cretaceous diatoms from Ocean Drilling Program (ODP) Leg 113 Site 693 (Weddell Sea). Part 1. Vegetative cells. *Proc. ODP Scientific Results* 113:365–402.
- Gomez, A. 2007. The consortium of the protozoan *Solenicola setigera* and the diatom *Leptocylindrus mediterraneus* in the Pacific Ocean. *Acta Protozool.* 46:15–24.
- Gran, H. H. 1915. *The Plankton Production in the North European Waters in the Spring of 1912*. Bureau du Conseil permanent international pour l'exploration de la mer, Paris, 142 pp.
- Guillard, R. L. & Ryther, J. H. 1962. Studies of marine planktonic diatoms. I. *Cyclotella nana* Hustedt, and *Detonula confervacea* (Cleve) Gran. *Can. J. Microbiol.* 8:229–39.
- Hall, T. 1999. BioEdit: a user-friendly biological sequence alignment editor and analysis program for Windows 95/98/NT. *Nucleic Acids Symp. Ser.* 41:95–8.
- Hargraves, P. E. 1990. Studies on marine plankton diatoms. V. Morphology and distribution on *Leptocylindrus minimus* Gran. *Nova Hedwigia Beih.* 100:47–60.
- Hasle, G. R. 1978. Diatoms. In Sournia, A. [Ed.] *Phytoplankton Manual*. UNESCO, Paris, pp. 136–42.
- Hasle, G. R. & Syvertsen, E. E. 1997. Marine diatoms. In Tomas, C. R. [Ed.] *Identifying Marine Phytoplankton*. Academic Press, San Diego, CA, pp. 5–385.
- Hendey, N. I. 1964. *An introductory Account of the Smaller Algae of British Coastal Waters. V. Bacillariophyceae (Diatoms)*. Her Majesty's Stationery Office, London, 317 pp.
- Hofacker, I., Fontana, W., Stadler, P., Bonhoeffer, S., Tacker, M. & Schuster, P. 1994. Fast folding and comparison of RNA secondary structures. *Monatsh. Chem.* 125:167–88.
- Huseby, S., Degerlund, M., Zingone, A. & Hansen, E. 2012. Metabolic fingerprinting reveals differences between northern and southern strains of the cryptic diatom *Chaetoceros socialis*. *Eur. J. Phycol.* 47:480–9.
- Huson, D. H. & Scornavacca, C. 2012. Dendroscope 3: an interactive tool for rooted phylogenetic trees and networks. *Syst. Biol.* 61:1061–7.
- Hustedt, F. 1962. *Die kieselalgen. Deutschlands, Österreichs und der Schweiz unter Berücksichtigung der übrigen Länder Europas sowie der angrenzenden Meeresgebiete. 3. Teil*. Akademische Verlagsgesellschaft m.b.h., Leipzig, 816 pp.
- Intergovernmental Oceanographic Commission (I.O.C) UNESCO. 2012. *The Ocean Biogeographic Information System (OBIS)*. Available at: <http://www.iobis.org> (accessed 10 November 2012).
- Keller, M. D., Selvin, R. C., Claus, W. & Guillard, R. R. L. 1987. Media for the culture of oceanic ultraphytoplankton. *J. Phycol.* 23:633–8.
- Kooistra, W. H. C. F., De Stefano, M., Medlin, L. K. & Mann, D. G. 2003. The phylogenetic position of *Toxarium*, a pennate-like lineage within centric diatoms (Bacillariophyceae). *J. Phycol.* 39:185–97.
- Kooistra, W. H. C. F., Sarno, D., Balzano, S., Gu, H., Andersen, R. A. & Zingone, A. 2008. Global diversity and biogeography of *Skeletonema* species (Bacillariophyta). *Protist* 159:177–93.
- Kooistra, W. H. C. F., Sarno, D., Hernández-Becerril, D. U., Assmy, P., Di Prisco, C. & Montresor, M. 2010. Comparative molecular and morphological phylogenetic analyses of taxa in the Chaetocerotaceae (Bacillariophyta). *Phycologia* 49:471–500.
- Kraberger, A., Baumann, M. & Dürsel, C. D. 2010. *Coastal Phytoplankton: Photo Guide for Northern European Seas*. Verlag Dr. Friedrich Pfeil, Munich, 204 pp.
- Lundholm, N., Bates, S. S., Baugh, K. A., Bill, B. D., Connell, L. B., Léger, C. & Trainer, V. L. 2012. Cryptic and pseudo-cryptic diversity in diatoms—with descriptions of *Pseudo-nitzschia hasleana* sp. nov. and *P. fryxelliana* sp. nov. *J. Phycol.* 48:436–54.
- Mann, D. G. & Droop, S. J. M. 1996. Biodiversity, biogeography and conservation of diatoms. *Hydrobiologia* 336:19–32.
- Meunier, A. 1915. *Microplankton de la Mer Flamande*. Mémoires du Musée Royal d'Histoire Naturelle de Belgique, VIII (3). Hayez, Imprimeur de l'Académie Royale de Belgique, Bruxelles, 7 plates, 118 pp.
- Montresor, M. & Lewis, J. 2006. Phases, stages, and shifts in the life cycles of marine phytoplankton. In Subba Rao, D. V. [Ed.] *Algal Cultures, Analogues of Blooms and Applications*. Science Publishers, Enfield, pp. 91–129.
- Murray, J., Appellöf, J. J. A., Gran, H. H., Helland-Hansen, B. & Hjort, J. 1912. *The Depths of the Ocean: A General Account of the Modern Science of Oceanography Based Largely on the Scientific Researches of the Norwegian Steamer Michael Sars in the North Atlantic/by Sir John Murray and Dr. Johan Hjort; with contributions from Professor A. Appellöf, Professor H. H. Gran and Dr. B. Helland-Hansen*. Macmillan, London, 821 pp.
- Nagai, S., Hori, Y., Manabe, T. & Imai, I. 1995. Restoration of cell size by vegetative cell enlargement in *Coscinodiscus wailesii* (Bacillariophyceae). *Phycologia* 34:533–5.
- Nanjappa, D. 2012. *Genetic, Physiological and Ecological Diversity in the Diatom Genus Leptocylindrus*. PhD thesis, The Open University, Milton Keynes, UK, 220 pp.
- Posada, D. & Crandall, K. A. 2001. Selecting the best-fit model of nucleotide substitution. *Syst. Biol.* 50:580–601.
- Rambaut, A. 1996–2002. Sequence Alignment Editor v2.0a11. Available at: <http://tree.bio.ed.ac.uk/software/seal/> (accessed August 5 2013).
- Ribera d'Alcalà, M., Conversano, F., Corato, F., Licandro, P., Mangoni, O., Marino, D., Mazzocchi, M. G. et al. 2004. Seasonal patterns in plankton communities in a pluriannual time series at a coastal Mediterranean site (Gulf of Naples): an attempt to discern recurrences and trends. *Sci. Mar.* 68:65–83.
- Rines, J. E. B. & Hargraves, P. E. 1990. Morphology and taxonomy of *Chaetoceros compressus* Lauder var. *hirtisetus* var. *nova*, with preliminary consideration of closely related taxa. *Diatom Res.* 5:113–27.
- Rivera, P., Cruces, F. & Clement, A. 2002. *Leptocylindrus minimus* Gran (Bacillariophyceae): morphology and distribution in Chile. *Gayana Bot.* 59:7–11.
- Round, F. E., Crawford, R. M. & Mann, D. G. 1990. *The Diatoms. Biology and Morphology of the Genera*. Cambridge University Press, Cambridge, 747 pp.

- Sarno, D., Kooistra, W. C. H. F., Balzano, S., Hargraves, P. E. & Zingone, A. 2007. Diversity in the genus *Skeletonema* (Bacillariophyceae): III. Phylogenetic position and morphological variability of *Skeletonema costatum* and *Skeletonema grevillei*, with the description of *Skeletonema ardens* sp. nov. *J. Phycol.* 43:156–70.
- Sarno, D., Kooistra, W. C. H. F., Medlin, L. K., Percopo, I. & Zingone, A. 2005. Diversity in the genus *Skeletonema* (Bacillariophyceae). II. An assessment of the taxonomy of *S. costatum*-like species, with the description of four new species. *J. Phycol.* 41:151–76.
- Schiller, J. 1929. Über eine biologische und hydrographische Untersuchung des Oberflächenwassers im westlichen Mittelmeer im August 1928. *Bot. Arch.* 27:381–419.
- Schröder, J. 1908. Neue und seltene Bacillariaceen aus dem Plankton der Adria. *Ber. Deut. Bot. Ges.* 26a:615–20.
- Skvortzow, B. V. 1931. Pelagic diatoms of Korean strait of the Sea of Japan. *Philipp. J. Sci.* 46:95–122, 10 pls.
- Smayda, T. J. 1963. A quantitative analysis of the phytoplankton of the Gulf of Panama. I. Results of the regional phytoplankton surveys during July and November 1957 and March, 1958. *Interamerican Trop. Tuna Comm. Bull.* 7:191–253.
- Sorhannus, U. 2004. Diatom phylogenetics inferred based on direct optimization of nuclear-encoded SSU rRNA sequences. *Cladistics* 20:487–97.
- Stamatakis, A. 2006. RAxML-VI-HPC: maximum likelihood-based phylogenetic analyses with thousands of taxa and mixed models. *Bioinformatics* 22:2688–90.
- von Stosch, H. A. 1965. Manipulierung der zellgröße von diatomeen in Experiment. *Phycologia* 5:21–44.
- Sunesen, I. & Sar, E. A. 2007. Diatomeas marinas de aguas costeras de la provincia de Buenos Aires (Argentina). III Géneros potencialmente nocivos *Asterionellopsis*, *Cerataulina*, *Ceratoneis* y *Leptocylindrus*. *Rev. Chil. Hist. Nat.* 80:493–507.
- Swofford, D. L. 1998. *PAUP**. *Phylogenetic Analysis Using Parsimony (* and other methods)*. Version 4.0b10. Sinauer Associates, Sunderland, MA.
- Theriot, E. C., Ashworth, M., Ruck, E., Nakov, T. & Jansen, R. K. 2010. A preliminary multigene phylogeny of the diatoms (Bacillariophyta): challenges for future research. *Plant Ecol. Evol.* 143:278–96.
- Thompson, J. D., Higgins, D. G. & Gibson, T. J. 1994. Clustal W: improving the sensitivity of progressive multiple sequence alignment through sequence weighting, position-specific gap penalties and weight matrix choice. *Nucleic Acids Res.* 22:4673–80.
- University of Yokohama. 2012. Microflora/fauna of Yokohama. Available at: http://www.biol.tsukuba.ac.jp/~algae/YMFF/Bacillariophyceae/Leptocylindrus_minimus/index.html (accessed November 13 2012).
- Zingone, A., Percopo, I., Sims, P. A. & Sarno, D. 2005. Diversity in the genus *Skeletonema* (Bacillariophyceae). I. A re-examination of the type material of *Skeletonema costatum*, with the description of *S. grevillei* sp. nov. *J. Phycol.* 41:140–50.

Supporting Information

Additional Supporting Information may be found in the online version of this article at the publisher's web site:

Figure S1. ML tree inferred from concatenated SSU rDNA-*rbL-psbC* sequences illustrating the relationship among *Tenuicylindrus*, *Leptocylindrus* species and other groups. *Bolidomonas pacifica* was included as outgroup. Bootstrap values have been generated with 1,000 replicates.

Figure S2. ML tree inferred from the nuclear SSU rDNA sequences of *Tenuicylindrus*, *Leptocylindrus*, other diatom genera and *Bolidomonas pacifica* as outgroup.

Figure S3. ML tree inferred from the *rbL* gene of *Tenuicylindrus*, *Leptocylindrus*, other diatom genera and *Bolidomonas pacifica* as outgroup.

Figure S4. ML tree inferred from the *psbC* gene of *Tenuicylindrus*, *Leptocylindrus*, other diatom genera and *Bolidomonas pacifica* as outgroup.

Table S1. Strains used in the analysis. All strains are from the Gulf of Naples, except CCMP 1856, which was isolated by P. Hargraves from the Gulf of Mexico.

Table S2. Oligonucleotide primers used to amplify and sequence nuclear rDNA regions (including SSU, partial LSU, 5.8S rDNA, and ITS), plastid SSU rDNA, *rbL*, and *psbC* fragments from *Leptocylindrus*.

Table S3. Light microscope morphometric characters in *Leptocylindrus* and *Tenuicylindrus* species.

Table S4. Electron microscope morphometric characters in *Leptocylindrus* species and *Tenuicylindrus belgicus*. All information is from culture material.

Table S5. DNA markers used in this study, their alignment lengths, and variable parsimony informative positions.

Table S6. Base composition and estimated base substitution models as inferred with Modeltest (Posada and Crandall 2001) for each of the alignments used in this study (UA: unalignable data).

Table S7. DNA sequence dissimilarities within the genus and/or to the closest genus.